Accepted Manuscript

Toward new classes of potent antibiotics: synthesis and antimicrobial activity of novel metallo-saldach-imidazolium salts

Reda F.M. Elshaarawy, Christoph Janiak

PII: S0223-5234(13)00602-8

DOI: 10.1016/j.ejmech.2013.09.029

Reference: EJMECH 6432

To appear in: *European Journal of Medicinal Chemistry*

Received Date: 16 May 2013

Revised Date: 17 July 2013

Accepted Date: 9 September 2013

Please cite this article as: R.F.M. Elshaarawy, C. Janiak, Toward new classes of potent antibiotics: synthesis and antimicrobial activity of novel metallo-saldach-imidazolium salts, *European Journal of Medicinal Chemistry* (2013), doi: 10.1016/j.ejmech.2013.09.029.

Toward new classes of potent antibiotics: synthesis and antimicrobial activity of novel metallo-saldach-imidazolium salts

Reda F.M. Elshaarawy,[a,b,*] and Christoph Janiak[b,*]

Graphical abstract:

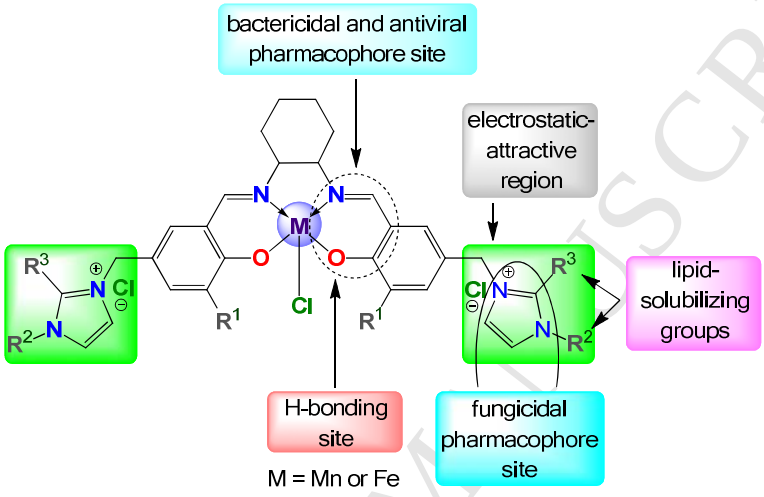

A novel synthetic strategy has been successfully developed for the synthesis of saldach-imidazolium derivatives and their complexes. These compounds represent promising candidates when set in the context of antimicrobial applications.

Toward new classes of potent antibiotics: synthesis and antimicrobial activity of novel metallo-saldach-imidazolium salts

Reda F.M. Elshaarawy,[a,b,*] and Christoph Janiak[b,*]

Highlights:

- *N*,*N*`-bis(salicylidene)-(±)-*trans*-1,2-diaminocyclohexane (saldach) as scaffold.
- Imidazolium salts (Im^{+}-$R^{2}R^{3}$-Cl^{-}) covalently attached to $H_2(R^{1})_2$saldach backbone.
- Compounds were tested against four bacterial pathogens and two fungal strains.
- Most compounds showed promising antibacterial activity.
- $H_2(^{t}Bu)_2$saldach(Im^{+}-HMe-Cl^{-})$_2$ and its Fe-complex are possible antibiotic candidates.

Toward new classes of potent antibiotics: synthesis and antimicrobial activity of novel metallo-saldach-imidazolium salts

Reda F.M. Elshaarawy,[a,b,*] and Christoph Janiak[b,*]

[a] Faculty of Science, Suez University, Suez, Egypt. Email: reda_elshaarawi@science.suez.edu.eg; Reda.El-Shaarawy@uni-duesseldorf.de

[b] Institut für Anorganische Chemie und Strukturchemie, Heinrich-Heine Universität Düsseldorf, 40204 Düsseldorf, Germany. Email: janiak@uni-duesseldorf.de

Abstract

Imidazolium salts (Im^+-R^2R^3-Cl^-) attached to the *N,N`*-bis(salicylidene)-(±)-*trans*-1,2-diaminocyclohexane (saldach) backbone (**4a-f**) have been designed and successfully applied for the synthesis of the corresponding mononuclear complexes with Mn(III) and Fe(III) ions. The molecular structures of the saldach ligands $H_2(R^1)_2$saldach$(Im^+$-R^2R^3-$Cl^-)_2$ (R^1 = H, *tert*-Bu,R^2 = H, Et, *n*-Bu, R^3 = H, Me) and their [M(III)Cl{$(R^1)_2$saldach$(Im^+$-R^2R^3-$Cl^-)_2$}] (M = Mn, Fe) complexes have been established. The free ligands exist as the phenol-OH and not as the zwitterionic (imine)N-$H^+\cdots^-$O(phenol) tautomer. Antimicrobial activity of the target compounds revealed higher potent antibacterial activity against *S. aureus, B. subtilis* while less effective against *E. coli* and *C. albicans* and inactivity against *A. flavus*. Compound (**4d**) and its Fe(III) complex (**6d**) exhibit remarkable extra-potent bactericidal activity.

Keywords: *N,N`*-bis(salicylidene)-1,2-diaminocyclohexane, Imidazolium chlorides, Complexes, Spectral study, Antimicrobial survey.

1. Introduction

Antibiotics have revolutionized the medical care in the ^{20}th century. With the discovery of antibiotics, people were convinced that infectious diseases might someday be wiped out. However, the emergence and spread of multidrug-resistant bacteria have made treatment of infectious diseases difficult and have become a serious medical problem [1,2]. For example, strains of *Salmonella enterica,* a leading cause of bacterial gastroenteritis, are no longer susceptible to front line antibiotics [3] and the distribution of methicillin-resistant *S. aureus* (MRSA) strains has increased [4]. Moreover, the high level of inherent antibiotic resistance in *P. aeruginosa* makes treatment of these infections problematic [5]. This has given urgency to research to develop a variety of interesting compounds as drugs

used in many fields. Several approaches for negating antibiotic resistance are currently being investigated, including inactivation of enzymes in essential metabolic pathways and inhibiting signal transduction systems [6,7]. These approaches involve the development of new antimicrobial drugs with modes of action that circumvent current resistance mechanisms [8,9].

Notably, the salen type compounds prepared by the condensation of *o*-hydroxyaldehydes and diamine such as 1,2-diaminocyclohexane (DACH, dach) present versatile steric, electronic and liphophilic properties [10]. Salen type compounds have tremendous potential for a host of pharmaceutical applications; their enormous effects on different models have raised serious possibilities recently for their use as starting materials in the synthesis of antibiotics, antiallergic, antiphlogistic and antitumor drugs [11,12,13]. Unparalleled attention has been devoted to these materials due to their low cost, ease of fabrication and their stability. A tautomeric equilibrium has been recognized in 2-hydroxy Schiff bases due to the existence of (phenol)O-H$^{\cdots}$N(imine) and (phenol)O$^{-\cdots+}$H-N(imine) type hydrogen bonds. This equilibrium can be shifted to the zwitterionic form due to external electric fields from additional ionic charges within the molecule and molecular packing (Scheme 1) [14]. Hydrogen bonding interactions play roles in preferential solvation and have been investigated because they are present in a large variety of chemical, biochemical and pharmacological events. In salen compounds, the imine nitrogen can acts as intramolecular hydrogen bond acceptor and the phenolic oxygen derivatives can act as intermolecular hydrogen bond acceptor. Moreover, the conjugation between metal ions and biologically active Schiff bases becomes a subject worthy of pursuit and has demonstrated great promise for their extensive applications in the enhancement of their biological and biomedical activities [13,15,16,17].

At the same time, salt formation of Active Pharmaceutical Ingredients (APIs) is an attractive and commonly used approach to overcome the problems of solubility and stability of APIs. There are many well-known examples where biological active cations and anions combine together and the resulted salt exhibits the therapeutic effects of both of its components [18]. Therefore, it is quite reasonable to think that imidazolium salt units (as common in ionic liquids (ILs)) could potentially be included in anti-cancer, anti-viral and other therapeutic agents/drugs. These ‘Therapeutic Ionic salts’ offer distinctly different properties than the non-ionic backbone. If there is a therapeutic response then the major advantage of ionic salts would be in managing/tuning their toxicity while tailoring the physiochemical and pharmacological properties necessary for desired therapeutic applications. Recently the *in vitro* anti-microbial, biodegradability [19] and anti-tumor

activities [20] of a series of imidazolium based ionic liquids were reported. The imidazolium salts examined exhibit broad activities against *cocci*, *rods* and *fungi*. Also the structure–activity relationship showed that chain length of *N*-3 alkyl substitution plays a significant role in the anti-tumor activity and cytotoxicity.

In a continuation of our earlier endeavor [21] to design and synthesize novel bioactive compounds, the present work reports the synthesis and characterization of new saldach-imidazolium salts (ionic compounds) and their metal complexes (Scheme 1). In view of the already known independent biological importance of metallosaldach compounds and imidazolium ILs, we also explore here the *in vitro* antimicrobial activity of Mn(III)- and Fe(III) saldach-imidazolium salt systems (Scheme 1) against two Gram-positive, two Gram-negative bacteria and two different fungi. These ionic salts may promise potential therapeutics to combat antibiotic resistance. Herein, Mn(III) and Fe(III) species have been chosen in this study due to their potential importance and useful applications in the biological field.

2. Experimental Section

2.1. Physical measurements

Melting point was measured using a BÜCHI Melting point B-540 apparatus; all melting points were measured in open glass capillary and values are uncorrected. Elemental analyses for C, H, N, were performed with a Perkin–Elmer 263 elemental analyzer. FT-IR spectra were recorded on a BRUKER Tensor-37 FT-IR spectrophotometer in the range 400–4000 cm^{-1} as KBr discs or in the 4000-550 cm^{-1} region with 2 cm^{-1} resolution with an ATR (attenuated total reflection) unit (Platinum ATR-QL, Diamond). For signal intensities the following abbreviations were used: br (broad), sh (sharp), w (weak), m (medium), s (strong), vs (very strong). UV/Vis spectra were measured at 25 °C in deionized water (H_2O) (10^{-5} mol/L) on a Shimadzu UV-2450 spectrophotometer using quartz cuvettes (1 cm). NMR-spectra were obtained with a Bruker Avance DRX200 (200 MHz for ^{1}H) or Bruker Avance DRX500 (500 MHz for ^{13}C) spectrometer with calibration to the residual proton solvent signal in DMSO-d_6 (^{1}H NMR: 2.52 ppm, ^{13}C NMR: 39.5 ppm), $CDCl_3$ (^{1}H NMR: 7.26 ppm, ^{13}C NMR: 77.16 ppm) against TMS with δ = 0.00 ppm. Multiplicities of the signals were specified s (singlet), d (doublet), t (triplet), q (quartet) or m (multiplet). The mass spectra of the synthesized sal-imidazolium, saldach-imidazolium chlorides and their complexes were acquired in the linear mode for positive ions on a BRUKER Ultraflex MALDI-TOF instrument equipped with a 337 nm nitrogen laser pulsing at a repetition rate of 10 Hz. The MALDI

matrix material (1,8-dihydroxy-9(10H)-anthracenone (dithranol, DIT) ($C_{14}H_{10}O_3$, M= 226.23)) was dissolved in chloroform at a concentration of 10 mg/mL. MALDI probes were prepared by mixing compound solutions (1 mg/mL in CH_2Cl_2) with the matrix solution (1:10, v/v) in a 0.5 mL Eppendorf® micro tube. Finally 0.5 μL of this mixture was deposited on the sample plate dried at room temperature and then analyzed. The molar conductance 10^{-3} M solution of various salts has been measured at ambient temperature with a digital conductivity meter (S30 SevenEasy™ conductivity, Mettler-Toledo Electronics, LLC, Polaris Parkway, Columbus). The overall accuracy of the conductance measurements was found to be ± 0.2%. Magnetic measurements of target complexes were carried out at room temperature using a Vibrating Sample Magnetometer (VSM), (Model PAR 155).

2.2. Materials and Syntheses

Chemicals were obtained from the following suppliers and used without further purification: salicylaldehyde (sal), 2-*tert*-butylphenol (2-^{t}BuPhOH), 1-ethylimidazole (1-Et-Im), 2-methylimidazole (2-Me-Im), (±)-trans-1,2-diaminocyclohexane (dach), tetrabutyl-ammonium bromide (^{t}Bu$_4$NBr), anhydrous magnesium dichloride ($MgCl_2$) and manganese(II) acetate tetrahydrate ($Mn(CH_3COO)_2{\cdot}4H_2O$) (Sigma–Aldrich), paraformaldehyde ($(CH_2O)_n$) (Roth), 1-butylimidazole (1-^{n}Bu-Im) (Alfa Aesar), triethyl amine (Et_3N) and anhydrous zinc chloride ($ZnCl_2$) (GRÜSSING GmbH) and iron(III) chloride hexahydrate ($FeCl_3{\cdot}6H_2O$) (Acros). 3-*tert*-Butyl-2-hydroxybenzaldehyde (**1b**) was synthesized from 2-*tert*-butylphenol as described previously [22] and obtained as a pale yellow oil (82% yield). It becomes dark green on storage. ^{1}H NMR (200 MHz, $CDCl_3$) δ (ppm): 11.87 (s, 1H, Ph-O**H**), 9.91 (s, 1H, **H**C=O), 7.58 (dd, 1H, J_{HH} = 1.66, 6.02 Hz, Ph-**H**), 7.44 (dd, 1H, J_{HH} = 1.69, 7.67 Hz, Ph-**H**), 6.99 (t, 1H, J_{HH} = 7.68 Hz, Ph-**H**), 1.48 (s, 9H, C(C**H$_3$**)$_3$).

2.2.1. 5-Chloromethyl-2-hydroxybenzaldehyde (**2a**):

This compound was synthesized from salicylaldehyde according to the classical chloromethylation procedure [23] modified with catalyst $ZnCl_2$, and hydrogen chloride gas atmosphere. In a typical synthesis, (17.5 g, 160 mmol) of salicylaldehyde was treated with 24 ml of 37% aqueous formaldehyde and (1.2 g, 8.8 mmol) of $ZnCl_2$ in 100 ml of concentrated hydrochloric acid. The mixture was stirred at room temperature under $HC1_g$ atmosphere ($HC1_g$ was generated in another system, connected to the reaction vessel, by dropping concentrated H_2SO_4 slowly on to solid NaCl) for 24 h. The white solid that separated from the reaction mixture was filtered, re-dissolved in diethyl ether, and the combined organic phases were washed several times with milli-Q water, till pH = 7 for washing liquor, and then dried

over sodium sulfate. Volatiles were distilled off, under inert atmosphere, and the resulting white crude residue was filtered and further recrystallized from *n*-hexane to furnish 5-chloromethyl-2-hydroxybenzaldehyde as white-colored needles (15.2 g, 62.0 % yield). FT-IR (ATR, cm^{-1}): 3240 (m, br, *v* OH), 3120 (m, br, v_{asym} CH, Ph), 3050 (m, br, v_{sym} CH, Ph), 2876 (m, sh, *v* CH_2), 1659 (vs, sh, *v* C=O), 1578, 1489, 1437 (s, sh, *v* $C=C_{arom}$ + *v* C-H bend), 1338 (m, sh, *v* CH_2), 1252 (s, sh, *v* CH_2Cl), 1150 (s, sh, *v* HCC, Ph), 772 (s, sh, *v* C–Cl). ^{1}H NMR (200 MHz, $CDCl_3$) δ (ppm): 11.07 (s, 1H, Ph-O**H**) 9.90 (s, 1H, Ph-**H**C=O), 7.59-7.55 (m, 2H, 2 x Ph-**H**), 7.02–6.98 (d, 1H, J_{HH} = 8.34 Hz, Ph-**H**), 4.60 (s, 2H, C$\mathbf{H_2}$-Ph). ^{13}C NMR (500 MHz, $CDCl_3$) δ (ppm): 196.02 (H**C**=O), 160.90 (**C**-OH), 137.22 (**C**, Ph), 133.64 (**C**H, Ph), 129.86 (**C**H, Ph), 120.34 (**C**, Ph), 118.72 (**C**H, Ph), 45.28 **C**H_2-phenyl).

2.2.2. 3-*tert*-Butyl-5-chloromethyl-2-hydroxybenzaldehyde (**2b**):

A mixture of **1b** (2.7 g, 15.2 mmol), $(CH_2O)_n$ (1.0 g, 33.3 mmol), and $^tBu_4NBr$ (0.47 g, 1.46 mmol) in 11 ml of concentrated hydrochloric acid was stirred vigorously at ambient temperature for 72 h [24]. The resulting emulsion was extracted with diethyl ether (3 × 25 mL). Then the organic phase was washed with saturated brine solution (2 × 10 ml), milli-Q water (5 × 10 ml) and, then dried over anhydrous magnesium sulfate. This extract was further concentrated under vacuum to give 3-*tert*-butyl-5-(chloromethyl)-2-hydroxybenzaldehyde **2b** as a pale yellow crystalline solid (1.99 g, 58% yield). FT-IR (ATR, cm^{-1}): 3428 (m, br, *v* OH), 3154 (m, br, v_{asym} CH, Ph), 3070 (m, br, v_{sym} CH, Ph), 2956 (m, sh, *v* CH_3), 2848 (m, sh, *v* CH_2), 1651 (vs, sh, *v* C=O), 1612, 1476, 1435 (s, sh, *v* $C=C_{arom}$ + *v* C-H bend), 1331 (m, sh, *v* CH_2), 1263 (s, sh, *v* CH_2Cl), 1172 (s, sh, *v* HCC, Ph), 694 (s, sh, C–Cl). ^{1}H NMR (200 MHz, $CDCl_3$) δ (ppm): 11.90 (s, 1H, Ph-O**H**) 9.91 (s, 1H, Ph-**H**C=O), 7.57-7.56 (d, H, J_{HH} = 2.29, Ph-**H**), 7.47-7.46 (d, 1H, J_{HH} = 2.27, Ph-**H**), 4.63 (s, 2H, C$\mathbf{H_2}$-Ph), 1.46 (s, 9H, C(C$\mathbf{H}_3$)$_3$). ^{13}C NMR (500 MHz, $CDCl_3$) δ (ppm): 192.98 (H**C**=O), 160.27 (**C**-OH), 136.88 (**C**, Ph), 133.78 (**C**H, Ph), 130.36 (**C**, Ph), 129.00 (**C**, Ph), 125.17 (**C**H, Ph), 46.06 (**C**H_2-Ph), 31.89 (**C**$(CH_3)_3$), 30.56 (C(**C**$H_3)_3$).

2.2.3. Preparation of salicylaldehyde-alkylimidazolium chlorides H(R^1)sal(Im^+-R^2R^3-Cl^-) (**3a-f**)

General method; To a vigorously stirred solution of imidazole derivatives (23.39 mmol) in dry toluene (10 mL) at room temperature was added the solution of chloromethyl-salicylaldehydes **2a,b** (19.50 mmol) in dry toluene (10 mL), drop-wise, under nitrogen atmosphere. The resulting solution was further stirred at 60 °C for 24 h. The product separated out was washed twice with toluene (2 x 5 mL) and several with ether (5 x 10 mL),

to remove the unreacted materials, and dried under vacuum to give pale yellow solid which used for the following preparations without further purification. Samples of the products were nevertheless isolated and fully characterized, as described below.

3-(3-Formyl-4-hydroxybenzyl)-2-methyl-1H-imidazol-3-ium chloride (**3a**): Obtained as pale yellow solid (4.48 g, 91%). FT-IR (KBr, cm^{-1}): 3364 (m, br, *v* N(1)-H and O-H), 3161 (m, br, v_{asym} CH, CH, Im and Ph), 3080 (m, br, v_{sym} CH, Im and Ph), 2979 (m, sh, v_{asym} CH_3), 2959 (m, sh, v_{sym} CH_3), 2884 (m, sh, *v* CH_2), 1661 (vs, sh, *v* C=O), 1573, 1485, 1455 (s, sh, *v* $C=C_{arom}$ + *v* C-H bend), 1338 (m, sh, *v* CH_2), 1149 (s, sh, HCC, HCN bending, Im), 823 (m, sh), 750 (m, sh), 682 (m, sh), 555 (m, sh). ^{1}H NMR (200 MHz, $CDCl_3$) δ (ppm): 10.83 (s, 1H, Ph-**H**C=O) 10.30 (s, 1H, Ph-O**H**), 10.15 (s, 1H, N-**H** Im), 7.86-7.81 (d, 1H, J_{HH} =1.39 Hz, N(1)CHC**H**- Im), 7.76-7.74 (d, J_{HH} = 1.41 Hz, 1H, N(1)C**H**CH- Im), 7.47.7.13 (m, 3H, 3 x Ph-**H**), 5.45 (s, 2H, -N(3)-C$\mathbf{H_2}$-Ph), 2.57 (s, 3H, C(2)-C$\mathbf{H_3}$). ^{13}C NMR (500 MHz, $CDCl_3$) δ (ppm): 196.89 (H**C**=O), 159.21 (**C**-OH), 144.8 (-N(1)**C**(CH_3)N(3)-), 136.68 (**C**-C=O), 136.47 (**C**H, Ph), 130.99 (**C**H, Ph), 127.35 (**C**, Ph), 122.74 ((-N(1)CH**C**H-), 122.41 (-N(1)**C**HCH-), 117.88 (**C**H, Ph), 51.88 (-N(1)**C**H_2.Ph), 22.73 (C(2)-**C**H_3). MALDI-TOF MS, *m/z*: 217.1 $[M - Cl]^+$.

1-Ethyl-3-(3-formyl-4-hydroxybenzyl)-1H-imidazol-3-ium chloride (**3b**): Obtained as yellow solid (3.56 g, 69 %). FT-IR (KBr, cm^{-1}): 3343 (m, br, *v* O-H), 3135 (m, br, v_{asym} CH, Im and Ph), 3098 (m, br, v_{sym} CH, Im and Ph), 2933 (m, sh, v_{asym} CH_3), 2908 (m, sh, v_{sym} CH_3), 2843 (m, sh, *v* CH_2), 1662 (vs, sh, *v* C=O), 1568, 1497, 1458 (s, sh, *v* $C=C_{arom}$ + *v* C-H bend), 1249 (m, sh, δ CH_3 + *v* N-CH_2), 1152 (s, sh, *v* HCC + *v* HCN bending, Im), 825 (m, sh), 759 (m, sh), 682 (m, sh), 558 (m, sh). ^{1}H NMR (200 MHz, $CDCl_3$) δ (ppm): 10.99 (s, 1H, Ph-**H**C=O), 10.29 (s, 1H, Ph-O**H**), 9.31 (s, 1H, -N(1)C**H**N(3)- Im), 7.83-7.81 (d, J_{HH} = 1.51 Hz, 1H, N(1)CHC**H**- Im), 7.77-7.75 (d, J_{HH} = 1.60 Hz, 1H, N(1)C**H**CH- Im), 7.69 (s, 1H, Ph-H), 7.59-7.57 (d, 1H, J_{HH} = 7.02 Hz, Ph-H), 7.18-7.16 (d, 1H, J_{HH} = 8.34 Hz, Ph-H), 5.36 (s, 2H, -N(3)-C$\mathbf{H_2}$-Ph), 4.16-4.12 (q, 2H, -N(1)C$\mathbf{H_2}$), 1.27-1.24 (t, J_{HH} = 7.30, 7.34 Hz, 3H, -CH_2C$\mathbf{H_3}$). ^{13}C NMR (500 MHz, $CDCl_3$) δ (ppm): 196.16 (H**C**=O), 158.98 (**C**-OH), 139.02 (-N(1)**C**HN(3)-), 136.17 (**C**-C=O), 136.06 (**C**H, Ph), 130.64 (**C**H, Ph), 126.89 (**C**, Ph), 123.00 ((-N(1)CH**C**H-), 122.92 (-N(1)**C**HCH-), 117.32 (**C**H, Ph), 53.68 (-N(1)**C**H_2-phenyl), 41.54 (N(1)-**C**H_2) , 15.79 (CH_3, CH_2-**C**H_3). MALDI-TOF MS, *m/z*: 231.1 $[M-Cl]^+$.

1-Butyl-3-(3-formyl-4-hydroxybenzyl)-1H-imidazol-3-ium chloride (**3c**): Obtained as yellow solid (4.90 g, 86%). FT-IR (KBr, cm^{-1}): 3359 (m, br, *v* O-H), 3185 (m, br, v_{asym} CH, Im and

Ph), 3066 (m, br, ν_{sym} CH, Im and Ph), 2981 (m, sh, ν_{asym} CH_3), 2960 (m, sh, ν_{sym} CH_3), 2877 (m, sh, ν CH_2), 1657 (vs, sh, ν C=O), 1569, 1552, 1469 (s, sh, ν $C=C_{arom}$ + ν C-H bend), 1336 (m, sh, δ CH_3 + δ CH_2), 1245 (m, sh, δ CH_3 + ν N-CH_2), 1149 (s, sh, ν HCC + ν HCN bending, Im), 850 (m, sh), 736 (m, sh), 679 (m, sh), 582 (m, sh). ^{1}H NMR (200 MHz, $CDCl_3$) δ (ppm): 11.37 (s, 1H, Ph-**H**C=O) 10.30 (s, 1H, Ph-O**H**), 9.53 (s, 1H, -N(1)C**H**N(3)- Im), 7.88-7.86 (d, 2H, N(1)C**H**C**H**- Im), 7.74 (s, 1H, Ph-H), 7.66-7.64 (d, 1H, J_{HH} =6.99 Hz, Ph-H), 7.26.7.24 (d, 1H, J_{HH} =8.56 Hz, Ph-H), 5.40 (s, 2H, -N(3)-C**H$_2$**-Ph), 4.20-4.17 (t, J_{HH} = 7.06, 7.14 Hz, 2H, -N(1)C**H$_2$**), 1.79-1.73 ($m_{(5)}$, 2H, -N(1)CH_2C**H$_2$**), 1.27-1.19 ($m_{(6)}$, 2H, -C**H$_2$**CH_3), 0.89-0.86 (t, J_{HH} = 7.33, 7.38 Hz, 3H, -CH_2C**H$_3$**). ^{13}C NMR (500 MHz, $CDCl_3$) δ (ppm): 195.81 (H**C**=O), 159.04 (**C**-OH), 138.51 (-N(1)**C**HN(3)-), 136.10 (**C**-C=O), 135.89 (**C**H, Ph), 130.96 (**C**H, Ph), 126.73 (**C**, Ph), 123.23 (-N(1)CH**C**H-), 123.02 (-N(1)**C**HCH-), 116.77 (**C**H, Ph), 53.74 (-N(1)**C**H_2-phenyl), 48.13 (N(1)-**C**H_2) , 34.79 (N(1)-CH_2-**C**H_2), 19.44 (-**C**H_2-CH_3), 13.40 (-CH_2-**C**H_3). MALDI-TOF MS, *m/z*: 259.2 $[M - Cl]^+$.

3-(3-(tert-Butyl)-5-formyl-4-hydroxybenzyl)-2-methyl-1H-imidazol-3-ium chloride (**3d**): Obtained as faint yellow semi-solid (3.65 g, 88 %). ^{1}H NMR (200 MHz, $CDCl_3$) δ (ppm): 11.91 (s, 1H, Ph-**H**C=O) 10.79 (s, 1H, Ph-O**H**), 9.91 (s, 1H, -N-**H** Im), 7.85-7.83 (d, 1H, J_{HH} =1.60 Hz, N(1)CHC**H**- Im), 7.55-7.54 (d, J_{HH} = 1.60 Hz, 1H, N(1)C**H**CH- Im), 7.27 (s, 1H, Ph-**H**), 7.01 (s, 1H, Ph-**H**), 5.53 (s, 2H, -N(3)-C**H$_2$**-Ph), 2.78 (s, 3H, C(2)-C**H$_3$**), 1.38 (s, 9H, C(C**H$_3$**)$_3$). ^{13}C NMR (500 MHz, $CDCl_3$) δ (ppm): 196.84 (H**C**=O), 160.26 (**C**-OH), 145.32 (-N(1)**C**(CH_3)N(3)-), 135.48 (**C**-C$(CH_3)_3$), 133.88 (**C**H, Ph), 129.06 (**C**, **C**-C=O), 127.24 (**C**H, Ph), 124.6 (**C**, Ph), 123.45 ((-N(1)CH**C**H-), 122.93 (-N(1)**C**HCH-), 52.00 (-N(1)**C**H_2-Ph), 34.41 (C-**C**$(CH_3)_3$), 29.97 (C-C(**C**H_3)$_3$), 18.52 (C(2)-**C**H_3), MALDI-TOF MS, *m/z*: 273.1 $[M - Cl]^+$.

3-(3-(tert-Butyl)-5-formyl-4-hydroxybenzyl)-1-ethyl-1H-imidazol-3-ium chloride ((**3e**): Obtained as yellow-orange wax (2.98 g, 58 %). ^{1}H NMR (200 MHz, $CDCl_3$) δ (ppm): 11.93 (s, 1H, Ph-**H**C=O) 9.98 (s, 1H, Ph-O**H**), 9.91 (s, 1H, -N(1)C**H**N(3)- Im), 7.86-7.84 (d, 1H, J_{HH} =1.59 Hz, N(1)CHC**H**- Im), 7.56-7.54 (d, J_{HH} = 1.63 Hz, 1H, N(1)C**H**CH- Im), 7.34 (s, 1H, Ph-**H**), 7.26 (s, 1H, Ph-**H**), 5.52 (s, 2H, -N(3)-C**H$_2$**-Ph), 4.22-4.11 (q, 2H, -N(1)C**H$_2$**), 1.39 (s, 9H, C(C**H$_3$**)$_3$), 1.26-1.20 (t, J_{HH} = 7.28, 7.30 Hz, 3H, -CH_2C**H$_3$**). ^{13}C NMR (500 MHz, $CDCl_3$) δ (ppm): 196.89 (H**C**=O), 155.73 (**C**-OH), 137.69 (**C**, Ph), 135.81 (-N(1)**C**HN(3)-), 133.23 (**C**H, Ph), 130.33 (**C**, **C**-C=O), 128.57 (**C**, Ph), 125.06(**C**H, Ph), 123.43 (-N(1)CH**C**H-), 122.02 (-N(1)**C**HCH-), 54.74 (-N(3)**C**H_2-Ph), 41.13 (N(1)-**C**H_2), 34.40 (**C**$(CH_3)_3$), 29.33 (C(**C**H_3)$_3$), 16.08 (CH_2**C**H_3). MALDI-TOF MS, *m/z*: 287.2 $[M - Cl]^+$.

3-(3-(tert-Butyl)-5-formyl-4-hydroxybenzyl)-1-butyl-1H-imidazol-3-ium chloride (**3f**): Obtained as yellow solid (3.88 g, 77%). FT-IR (KBr, cm^{-1}): 3465 (m, br, *v* O-H), 3101 (m, br, v_{sym} CH, Im and Ph), 2976 (m, sh, v_{asym} CH_3), 2942 (m, sh, v_{sym} CH_3), 2883 (m, sh, *v* CH_2), 1650 (vs, sh, *v* C=O), 1541, 1477, 1445 (s, sh, *v* C=C_{arom} + *v* C-H bend), 1333 (m, sh, *v* CH_2), 1162 (s, sh, HCC, HCN bending, Im), 851 (m, sh), 749 (m, sh), 679 (m, sh), 558 (m, sh). ^{1}H NMR (200 MHz, $CDCl_3$) δ (ppm): 11.88 (s, 1H, Ph-**H**C=O) 10.11 (s, 1H, Ph-O**H**), 9.83 (s, 1H, -N(1)C**H**N(3)- Im), 7.87-7.86 (d, 2H, N(1)C**H**C**H**- Im), 7.60-7.57 (d, 1H, J_{HH} =7.01 Hz, Ph-**H**), 7.25-7.21 (d, 1H, J_{HH} =8.55 Hz, Ph-**H**), 5.49 (s, 2H, -N(3)-C$\mathbf{H_2}$-Ph), 4.09-3.97 (t, J_{HH} = 7.02, 6.99 Hz, 2H, -N(1)C$\mathbf{H_2}$), 1.69-1.65 ($m_{(5)}$, 2H, -N(1)CH_2C$\mathbf{H_2}$), 1.31 (s, 9H, C(C$\mathbf{H_3}$)$_3$), 1.28-1.20 ($m_{(6)}$, 2H, -C$\mathbf{H_2}$$CH_3$), 0.92-0.89 (t, J_{HH} = 7.18, 7.17 Hz, 3H, -CH_2C$\mathbf{H_3}$). MALDI-TOF MS, *m/z*: 315.2 $[M - Cl]^+$.

2.2.4. General procedure for the preparation of salen ligands $H_2(R^1)_2$saldach(Im^+-R^2R^3-Cl^-)$_2$ (**4a-f**):

A methanolic solution (10 mL) of (±)-*trans*-1,2-diaminocyclohexane (dach) (0.23 g, 2.0 mmol), in a Schlenk tube, was added drop wise to a methanolic solution (20 mL) of substituted salicylaldehyde-imidazolium salt H(R^1)sal(Im^+-R^2R^3-Cl^-) **3a-f** (4.0 mmol) into a 100 ml Schlenk flask under nitrogen atmosphere. The reaction mixture was stirred at 60 °C overnight. MeOH was partially removed under reduced pressure on a rotary evaporator, and the yellow products of **4a-f** were precipitated by ethyl acetate and kept in the refrigerator overnight. The precipitate was sonicated with Et_2O (3 x 25 mL), collected by filtration and dried under vacuum.

N,N'-Bis[5-((2-methylimidazolium)methylene)-salicylidene)-trans-1,2-cyclohexanediamine dichloride (**4a**): Yellow-orange powder, (2.16 g, 87 %). FT-IR (KBr, cm^{-1}): 3395 (m, br, *v* N(1)-H + *v* O-H), 3186 (w, br, v_{asym} CH, CH, Im and Ph), 3090 (m, br, v_{sym} CH, Im and Ph), 2941 (m, sh, *v* CH_3), 2861 (m, sh, *v* CH_2), 1630 (vs, sh, *v* C=N), 1558, 1475, 1443 (s, sh, *v* C=C_{arom} + *v* C-H bend), 1320 (m, sh, *v* CH_2), 1258 (m, sh, *v* Ph-O), 1160 (s, sh, *v* HCC + *v* HCN bending, Im). ^{1}H NMR (200 MHz, $CDCl_3$) δ (ppm): 13.30 (br, s, 2H, Ph-O**H**), 9.48 (s, 2H, Im-N**H**), 8.62 (s, 2H, 2 x **H**-C=N), 7.86-7.84 (d, 2H, J_{HH} =1.76 Hz, 2 x N(1)CHC**H**- Im), 7.63-7.62 (d, J_{HH} = 2.02 Hz, 2H, 2 x N(1)C**H**CH- Im), 7.58-7.42 (m, 4H, 4 x Ph-**H**), 6.92-6.84 (m, 2H, 2 x Ph-**H**), 5.30 (s, 4H, 2 x -N(3)-C$\mathbf{H_2}$-Ph), 3.95-3.83 (m, 2H, 2 x Cyhex-**H**), 3.38 (s, 6H, 2 x Im-C$\mathbf{H_3}$), 1.79-1.42 (m, 8H, 8 x Cyhex-**H**). MALDI-TOF MS, *m/z*: 659.4 $[M{\cdot}2H_2O+K]^+$; HRMS (ESI): *m/z*: calcd for $C_{30}H_{36}N_6O_2{\cdot}2H_2O$: 547.3835 $[M{\cdot}2H_2O-2Cl]^+$;

found: 547.3745. Anal. Calcd. for $C_{30}H_{36}Cl_2N_6O_2 \cdot 2H_2O$ (M = 619.58): C, 58.16; H, 6.51; N, 13.56; Found: C, 57.84; H, 6.23; N, 13.51. Conductivity = 284 μS/cm.

N,N'-Bis[5-((1-ethylimidazolium)methylene)-salicylidene)-trans-1,2-cyclohexanediamine dichloride (**4b**): Yellow powder, (2.51 g, 81 %). FT-IR (KBr, cm^{-1}): 3434 (s, br, *v* O-H), 3133 (w, br, v_{asym} CH, CH, Im and Ph), 3068 (m, br, v_{sym} CH, Im and Ph), 2933 (m, sh, *v* CH_3), 2858 (m, sh, *v* CH_2), 1632 (vs, sh, *v* C=N), 1569, 1497, 1447 (s, sh, *v* $C=C_{arom}$ + *v* C-H bend), 1349 (m, sh, *v* CH_2), 1253 (m, sh, *v* Ph-O), 1155 (s, sh, HCC, HCN bending, Im), 846, 761, 662. ^{1}H NMR (200 MHz, $CDCl_3$) δ (ppm): 13.48 (br, s, 2H, Ph-O**H**) 9.53 (s, 2H, N(1)C**H**N(3)- Im), 8.42 (s, 2H, 2 x **H**-C=N), 7.80-7.77 (d, 2H, J_{HH} =1.96 Hz, 2 x N(1)CHC**H**- Im), 7.50-7.48 (d, J_{HH} = 2.12 Hz, 2H, 2 x N(1)C**H**CH- Im), 7.36-7.29 (m, 4H, 4 x Ph-**H**), 6.98-6.93 (m, 2H, 2 x Ph-**H**), 5.36 (s, 4H, 2 x -N(3)-C**H$_2$**-Ph), 4.02-3.93 (q, 4H, 2 x -N(1)C**H$_2$**), 3.84-3.75 (m, 2H, 2 x Cyhex-**H**), 1.85-1.42 (m, 8H, 8 x Cyhex-**H**), 1.28-1.25 (t, J_{HH} = 6.99, 7.01 Hz, 6H, 2 x -CH_2C**H$_3$**). MALDI-TOF MS, *m/z*: 669.3 $[M \cdot H_2O+K]^+$ and 573.3 $[M - Cl]^+$. Anal. Calcd. for $C_{32}H_{40}Cl_2N_6O_2 \cdot H_2O$ (M = 629.62): C, 61.04; H, 6.72; N, 13.35; Found: C, 60.73; H, 6.33; N, 13.20. Conductivity = 265 μS/cm.

N,N'-Bis[5-((1-n-butylidazolium)methylene)-salicylidene)-trans-1,2-cyclohexane-diamine dichloride (**4c**): Pale yellow powder, (2.19 g, 77 %). FT-IR (KBr, cm^{-1}): 3398 (m, br, *v* O-H), 3140 (w, br, v_{asym} CH, CH, Im and Ph), 3022 (m, br, v_{sym} CH, Im and Ph), 2959 (m, sh, *v* CH_3), 2888 (m, sh, *v* CH_2), 1629 (vs, sh, *v* C=N), 1573, 1487, 1438 (s, sh, *v* $C=C_{arom}$ + *v* C-H bend), 1346 (m, sh, *v* CH_2), 1260 (m, sh, *v* Ph-O), 1158 (s, sh, HCC, HCN bending, Im), 843, 679, 561. ^{1}H NMR (200 MHz, $CDCl_3$) δ (ppm): 13.35 (br, s, 2H, 2 x Ph-O**H**) 9.63 (s, 2H, 2 x N(1)C**H**N(3)- Im), 8.28 (s, 2H, 2 x **H**-C=N), 7.76-7.73 (d, 2H, J_{HH} =1.87 Hz, 2 x N(1)CHC**H**-Im), 7.65-7.63 (d, J_{HH} = 1.89 Hz, 2H, 2 x N(1)C**H**CH- Im), 7.18-6.96 (m, 6H, 6 x Ph-**H**), 5.34 (s, 4H, 2 x -N(3)-C**H$_2$**-Ph), 4.24-4.17 (t, J_{HH} = 7.08, 7.09 Hz, 4H, 2 x -N(1)C**H$_2$**), 4.00-3.95 (m, 2H, 2 x Cyhex-**H**), 1.92-1.76 (m, 8H, 8 x Cyhex-**H**), 1.65-1.57 ($m_{(5)}$, 4H, 2 x -N(1)CH_2C**H$_2$**), 1.29-1.19 ($m_{(6)}$, 4H, 2 x -C**H$_2$**CH_3), 0.98-0.90 (t, J_{HH} = 7.05, 7.14 Hz, 6H, 2 x -CH_2C**H$_3$**). MALDI-TOF MS, *m/z*: 750.5 $[M \cdot 2.5H_2O+K]^+$ and 631.3 $[M - Cl]^+$. Anal. Calcd. for $C_{36}H_{48}Cl_2N_6O_2 \cdot 2.5H_2O$ (M = 712.75): C, 60.66; H, 7.50; N, 10.02; Found: C, 60.62; H, 7.35; N, 9.60. Conductivity = 239 μS/cm.

N,N'-Bis[3-tert-butyl-5-((2-methylimidazolium)methylene)-salicylidene)-trans-1,2-cyclo-hexandiamine dichloride (**4d**): Canary yellow solid, (2.17 g, 76 %). FT-IR (KBr, cm^{-1}): 3430 (m, br, *v* O-H), 3295 (m, br, *v* N(1)-H), 3086 (w, br, v_{asym} CH, CH, Im and Ph), 2997 (m, br,

ν_{sym} CH, Im and Ph), 2943 (m, sh, ν CH_3), 2868 (m, sh, ν CH_2), 1629 (vs, sh, ν C=N), 1593, 1476, 1443 (s, sh, ν $C=C_{arom}$ + ν C-H bend), 1360 (m, sh, ν CH_2), 1281 (m, sh, ν Ph-O), 1149 (s, sh, HCC, HCN bending, Im), 897, 868, 775, 700, 655, 510. ^{1}H NMR (200 MHz, $CDCl_3$) δ (ppm): 13.75 (br, s, 2H, 2 x Ph-O**H**) 10.05 (s, 2H, 2 x N-**H** Im), 8.28 (s, 2H, 2 x **H**-C=N), 7.65-7.64 (d, 2H, J_{HH} =1.93 Hz, 2 x N(1)CHC**H**- Im), 7.41-7.39 (d, J_{HH} = 1.99 Hz, 2H, 2 x N(1)C**H**CH- Im), 7.16-6.99 (m, 4H, 4 x Ph-**H**), 5.32 (s, 4H, 2 x -N(3)-C$\mathbf{H_2}$-Ph), 3.60-3.56 (m, 2H, 2 x Cyhex-**H**), 2.93 (s, 6H, 2 x C(2)-C$\mathbf{H_3}$), 1.83-1.45 (m, 8H, 8 x Cyhex-**H**), 1.22 (s, 18H, 2 x C(C$\mathbf{H_3}$)$_3$). MALDI-TOF MS, *m/z*: 736.5 $[M{\cdot}H_2O+Na]^+$ and 578.1 $[M{\cdot}H_2O-Cl]^+$. Anal. Calcd. for $C_{38}H_{52}Cl_2N_6O_2{\cdot}H_2O$ (M = 713.78): C, 63.94; H, 7.63; N, 11.77; Found: C, 64.12; H, 7.56; N, 11.48. Conductivity = 258 μS/cm.

N,N'-Bis[3-tert-butyl-5-((1-ethylimidazolium)methylene)-salicylidene)-trans-1,2-cyclohexane-diamine dichloride (**4e**): Pale yellow-orange powder, (2.00 g, 69 %). FT-IR (KBr, cm^{-1}): 3446 (m, br, ν O-H), 3090 (w, br, ν_{asym} CH, CH, Im and Ph), 3005 (m, br, ν_{sym} CH, Im and Ph), 2954 (m, sh, ν CH_3), 2865 (m, sh, ν CH_2), 1634 (vs, sh, ν C=N), 1591, 1479, 1439 (s, sh, ν $C=C_{arom}$ + ν C-H bend), 1362 (m, sh, ν CH_2), 1285 (m, sh, ν Ph-O), 1138 (s, sh, HCC, HCN bending, Im), 939, 828, 772, 711, 644. ^{1}H NMR (200 MHz, $CDCl_3$) δ (ppm): 13.68 (br, s, 2H, 2 x Ph-O**H**) 10.03 (s, 2H, 2 x N(1)C**H**N(3)- Im), 8.42 (s, 2H, 2 x **H**-C=N), 7.58-7.56 (d, 2H, J_{HH} =1.93 Hz, 2 x N(1)CHC**H**- Im), 7.39-7.37 (d, J_{HH} = 1.99 Hz, 2H, 2 x N(1)C**H**CH- Im), 7.26-6.98 (m, 4H, 4x Ph-**H**), 5.22 (s, 4H, 2 x -N(3)-C$\mathbf{H_2}$-Ph), 4.58-4.53 (q, 4H, 2 x N(1)C$\mathbf{H_2}$), 3.55-3.49 (m, 2H, 2 x Cyhex-**H**), 1.89-1.44 (m, 8H, 8 x Cyhex-**H**), 1.39 (s, 18H, 2 x C(C$\mathbf{H_3}$)$_3$), 1.24-1.20 (t, J_{HH} = 7.28, 7.30 Hz, 6H, 2 x -CH_2C$\mathbf{H_3}$). MALDI-TOF MS, *m/z*: 671.4 $[M{\cdot}H_2O-2Cl]^+$. Anal. Calcd. for $C_{40}H_{56}Cl_2N_6O_2{\cdot}H_2O$ (M = 741.83): C, 64.76; H, 7.88; N, 11.33; Found: C, 64.45; H, 7.83; N, 11.00. Conductivity = 239 μS/cm.

N,N'-Bis[3-tert-butyl-5-((1-butylimidazolium)methylene)-salicylidene)-trans-1,2-cyclohexane-diamine dichloride (**4f**): Yellow-orange solid, (2.07 g, 65 %). FT-IR (KBr, cm^{-1}): 3486 (m, br, ν O-H), 3055 (w, br, ν_{asym} CH, CH, Im and Ph), 2999 (m, br, ν_{sym} CH, Im and Ph), 2948 (m, sh, ν CH_3), 2880 (m, sh, ν CH_2), 1635 (vs, sh, ν C=N), 1560, 1478, 1444 (s, sh, ν $C=C_{arom}$ + ν C-H bend), 1366 (m, sh, ν CH_2), 1284 (m, sh, ν Ph-O), 1176 (s, sh, HCC, HCN bending, Im), 1284 (m, sh, ν Ph-O), 851, 772, 646. ^{1}H NMR (200 MHz, $CDCl_3$) δ (ppm): 13.73 (br, s, 2H, 2 x Ph-O**H**) 9.99 (s, 2H, 2 x N(1)C**H**N(3)- Im), 8.68 (s, 2H, 2 x **H**-C=N), 7.60-7.59 (d, 2H, J_{HH} =1.90 Hz, 2 x N(1)CHC**H**- Im), 7.41-7.39 (d, J_{HH} = 1.89 Hz, 2H, 2 x N(1)C**H**CH- Im), 7.26-7.00 (m, 4H, 4x Ph-**H**), 5.28 (s, 4H, 2 x -N(3)-C$\mathbf{H_2}$-Ph), 4.32-4.29 (t, J_{HH} = 6.99, 7.01 Hz,

4H, 2 x -N(1)C**H$_2$**), 3.48-3.43 (m, 2H, 2 x Cyhex-**H**), 1.92-1.70 (m, 8H, 8 x Cyhex-**H**), 1.63-1.55 ($m_{(5)}$, 4H, 2 x -N(1)CH$_2$C**H$_2$**), 1.36 (s, 18H, 2 x C(C**H$_3$**)$_3$), 1.28-1.19 ($m_{(6)}$, 4H, 2 x -C**H$_2$**CH$_3$), 1.00-0.96 (t, J_{HH} = 7.12, 7.12 Hz, 6H, 2 x -CH$_2$C**H$_3$**). MALDI-TOF MS, *m/z*: 762.2 $[M{\cdot}H_2O\text{-}Cl]^+$. Anal. Calcd. for $C_{44}H_{64}Cl_2N_6O_2{\cdot}H_2O$ (M = 797.94): C, 66.23; H, 8.34; N, 10.53; Found: C, 66.30; H, 8.33; N, 10.10. Conductivity = 220 μS/cm.

2.2.5. General procedure for the preparation of metallosaldach-imidazolium systems [M(III)Cl{$(R^1)_2$saldach(Im^+-R^2R^3-$Cl^-)_2$}] (M = Mn, Fe) (**5,6a-f**):

2.2.5.1. *Synthesis of Mn(III) complexes* (**5a-f**):

A yellow solution of the substituted imidazolium-saldach ligand $H_2(R^1)_2$saldach(Im^+-R^2R^3-$Cl^-)_2$ **4a-f** (0.9 mmol) in ethanol (10 mL) was degassed for 15 minutes. An ethanolic solution (5 mL) of Mn(OAc)$_2{\cdot}4H_2O$ (269 mg, 1.1 mmol) was then added with the yellow solution turning dark brown immediately, and the reaction mixture was refluxed for 2 hours under N_2. LiCl (69.9 mg, 1.65 mmol) was then added and the solution was refluxed for an additional 2 h with air bubbled through the solution. After evaporating the solvent under reduced pressure, the residue was re-dissolved in **CH_2Cl_2** (3 ml), over-layered ethyl acetate (3 ml) and the mixture kept in a refrigerator overnight. The precipitated solid was filtered off and washed with ethyl acetate and diethyl ether. Recrystallization from **CH_2Cl_2**/n-hexane yielded pure [Mn(III)Cl{$(R^1)_2$saldach(Im^+-R^2R^3-$Cl^-)_2$}] **5a-f**.

Chlorido-trans-[[2,2`-][(1,2-cyclohexanediyl) bis(nitrilomethylidyne)] bis[4-((2-methyl-imidazolium)methylene-phenolato]-[N,N`,O,O`] manganese(III) dichloride (**5a**): Dark-brown powder (556 mg, 92 %). FT-IR (KBr, cm^{-1}): 3286 (m, br, *v* N(1)-H), 3133 (w, br, v_{asym} CH, CH, Im and Ph), 2934 (m, sh, *v* CH_3), 2859 (m, sh, *v* CH_2), 1618 (vs, sh, *v* C=N), 1559, 1472, 1436 (s, sh, *v* C=C_{arom} + *v* C-H bend), 1348 (m, sh, *v* CH_2), 1275 (m, sh, *v* Ph-O), 1167 (s, sh, *v* HCC + *v* HCN bending, Im), 826 (m, sh, *v* Mn-N). MALDI-TOF MS, *m/z*: 710.9 $[M+K]^+$. Anal. Calcd. for $C_{30}H_{34}Cl_3MnN_6O_2$ (M = 671.93): C, 53.63; H, 5.10; N, 12.51; Found: C, 53.92; H, 5.02; N, 12.29. Conductivity = 351 μS/cm; μ_{eff} = 4.97 μ_B.

Chlorido-trans-[[2,2`-][(1,2-cyclohexanediyl) bis(nitrilomethylidyne)] bis[4-((1-ethylimidazo-lium)methylene-phenolato]-[N,N`,O,O`] manganese(III) dichloride monohydrate (**5b**$\cdot H_2O$): Brown powder (575 mg, 89 %). FT-IR (KBr, cm^{-1}): FT-IR (KBr, cm^{-1}): 3426 (s, br, *v* O-H H_2O), 3134 (w, br, v_{asym} CH, CH, Im and Ph), 3078 (m, br, v_{sym} CH, Im and Ph), 2934 (m, sh, *v* CH_3), 2858 (m, sh, *v* CH_2), 1621 (vs, sh, *v* C=N), 1558, 1439 (s, sh, *v*

C=C_{arom} + *v* C-H bend), 1346 (m, sh, *v* CH_2), 1273 (m, sh, *v* Ph-O), 1152 (s, sh, HCC, HCN bending, Im), 821 (m, sh, *v* Mn-N), 471 (m, sh, *v* Mn-O). MALDI-TOF MS, *m/z*: 722.3 $[M+Na]^+$. Anal. Calcd. for $C_{32}H_{38}Cl_2MnN_6O_2 \cdot H_2O$ (Mw = 718.00): C, 53.53; H, 5.62; N, 11.70; Found: C, 53.83; H, 5.41; N, 11.68. Conductivity = 335 μS/cm; μ_{eff} = 4.95 μ_B.

Chlorido-trans-[[2,2'-][(1,2-cyclohexanediyl) bis(nitrilomethylidyne)] bis[4-((1-butylimidazo-lium)methylene-phenolato]-[N,N',O,O'] manganese(III) dichloride monohydrate (**5c**·H_2O): Reddish-brown powder (599 mg, 86 %). FT-IR (KBr, cm^{-1}): 3436 (m, br, *v* O-H H_2O), 3129 (w, br, v_{asym} CH, CH, Im and Ph), 2935 (m, sh, *v* CH_3), 2859 (m, sh, *v* CH_2), 1614 (vs, sh, *v* C=N), 1547, 1500, 1446 (s, sh, *v* C=C_{arom} + *v* C-H bend), 1347 (m, sh, *v* CH_2), 1272 (m, sh, *v* Ph-O), 1152 (s, sh, HCC, HCN bending, Im) , 826 (m, sh, *v* Mn-N), 468 (m, sh, *v* Mn-O). MALDI-TOF MS, *m/z*: 796.8 $[M \cdot H_2O+Na]^+$. Anal. Calcd. for $C_{36}H_{46}Cl_3MnN_6O_3 \cdot H_2O$ (M = 774.10): C, 55.86; H, 6.25; N, 10.86; Found: C, 56.01; H, 6.26; N, 10.84. Conductivity = 307 μS/cm; μ_{eff} = 4.96 μ_B.

Chlorido-trans-[[2,2'-][(1,2-cyclohexanediyl) bis(nitrilomethylidyne)] bis[4-((2-methyl-imidazolium)methylene) -6-(t-Bu-phenolato]-[N,N',O,O'] manganese(III) dichloride monohydrate (**5d**·H_2O): Brown solid (657 mg, 91 %). FT-IR (KBr, cm^{-1}): 3411 (m, br, *v* O-H H_2O), 3294 (m, br, *v* N(1)-H), 2995 (w, br, v_{asym} CH, CH, Im and Ph), 2941 (m, sh, *v* CH_3), 2860 (m, sh, *v* CH_2), 1616 (vs, sh, *v* C=N), 1560, 1475, 1442 (s, sh, *v* C=C_{arom} + *v* C-H bend), 1356 (m, sh, *v* CH_2), 1295 (m, sh, *v* Ph-O), 1142 (s, sh, *v* HCC + *v* HCN bending, Im), 820 (m, sh, *v* Mn-N), 465(m, sh, *v* Mn-O). MALDI-TOF MS, *m/z*: 824.9 $[M \cdot H_2O+Na]^+$. Anal. Calcd. for $C_{38}H_{50}Cl_3MnN_6O_2 \cdot H_2O$ (M = 802.15): C, 56.90; H, 6.53; N, 10.48; Found: C, 57.10; H, 6.43; N, 10.30. Conductivity = 327 μS/cm; μ_{eff} = 4.89 μ_B.

Chlorido-trans-[[2,2'-][(1,2-cyclohexanediyl) bis(nitrilomethylidyne)] bis[4-((1-ethylimidazol- ium)methylene) -6-(t-Bu-phenolato]-[N,N',O,O'] manganese(III) dichloride monohydrate (**5e**·H_2O): Greenish-brown solid (672 mg, 90 %). FT-IR (KBr, cm^{-1}): 3388 (m, br, *v* O-H H_2O), 2997 (w, br, v_{asym} CH, CH, Im and Ph), 2953 (m, sh, *v* CH_3), 2860 (m, sh, *v* CH_2), 1622 (vs, sh, *v* C=N), 1585, 1475, 1440 (s, sh, *v* C=C_{arom} + *v* C-H bend), 1361 (m, sh, *v* CH_2), 1298 (m, sh, *v* Ph-O), 1136 (s, sh, *v* HCC + *v* HCN bending, Im), 819 (m, sh, *v* Mn-N), 463(m, sh, *v* Mn-O). MALDI-TOF MS, *m/z*: 830.6 $[M \cdot H_2O+H]^+$. Anal. Calcd. for $C_{40}H_{54}Cl_3MnN_6O_2 \cdot H_2O$ (M = 830.21): C, 57.87; H, 6.80; N, 10.12; Found: C, 58.09; H, 6.76; N, 10.12. Conductivity = 307 μS/cm; μ_{eff} = 4.87 μ_B.

Chlorido-trans-[[2,2'-][(1,2-cyclohexanediyl) bis(nitrilomethylidyne)] bis[4-((1-butylimidazol- ium)methylene) -6-(t-Bu-phenolato]-[N,N',O,O'] manganese(III) dichloride (**5f**): Faint-brown solid (680 mg, 87 %). FT-IR (KBr, cm^{-1}): 3000 (w, br, *v* CH, Im and Ph), 2947 (m, sh, *v* CH_3), 2877 (m, sh, *v* CH_2), 1623 (vs, sh, *v* C=N), 1558, 1475, 1441 (s, sh, *v* $C=C_{arom}$ + *v* C-H bend), 1360 (m, sh, *v* CH_2), 1293 (m, sh, *v* Ph-O), 1178 (s, sh, *v* HCC + *v* HCN bending, Im), 825 (m, sh, *v* Mn-N), 468 (m, sh, *v* Mn-O). MALDI-TOF MS, *m/z*: 832.3 $[M\text{-}Cl]^+$. Anal. Calcd. for $C_{44}H_{62}Cl_3MnN_6O_2$ (Mw = 868.30): C, 60.86; H, 7.20; N, 9.68; Found: C, 60.66; H, 7.24; N, 9.55. Conductivity = 291 μS/cm; μ_{eff} = 4.86 μ_B.

2.2.5.2 *Synthesis of Fe(III) complexes* (**6a-f**):

A yellow solution of the substituted imidazolium-saldach ligand $H_2(R^1)_2$saldach(Im^+-R^2R^3-$Cl^-)_2$ **4a-f** (0.9 mmol) in ethanol (10 mL) was degassed for 15 minutes. An ethanolic solution (5 mL) of $FeCl_3{\cdot}6H_2O$ (178 mg, 1.1 mmol) was then added with the yellow solution turning dark reddish-brown immediately, and the reaction mixture was refluxed for 2 hours under N_2. Then, the solution was concentrated and the residue was kept in a refrigerator overnight. The precipitated solid was filtered off and washed with cold ethanol (2 x 3mL) and diethyl ether (3 x 3mL) to yield [Fe(III)Cl{$(R^1)_2$saldach(Im^+-R^2R^3-$Cl^-)_2$}] **6a-f**.

Chlorido-trans-[[2,2'-][(1,2-cyclohexanediyl) bis(nitrilomethylidyne)] bis[4-((2-methylimidaz-olium)methylene)-phenolato]-[N,N',O,O'] iron(III) dichloride dihydrate (**6a**$\cdot 2H_2O$): reddish-brown powder (548, mg, 86 %). FT-IR (KBr, cm^{-1}): 3408 (m, br, *v* N(1)-H + *v* O-H H_2O), 3154 (w, br, v_{asym} CH, CH, Im and Ph), 2933 (m, sh, *v* CH_3), 2862 (m, sh, *v* CH_2), 1617 (vs, sh, *v* C=N), 1559, 1441 (s, sh, *v* $C=C_{arom}$ + *v* C-H bend), 1349 (m, sh, *v* CH_2), 1279 (m, sh, *v* Ph-O), 1166 (s, sh, *v* HCC + *v* HCN bending, Im), 817 (m, sh, *v* Fe-N). MALDI-TOF MS, *m/z*: 709.2 $[M{\cdot}2H_2O{+}H]^+$. Anal. Calcd. for $C_{30}H_{34}FeN_6O_2{\cdot}2H_2O$ (M = 708.86): C, 50.83; H, 5.40; N, 11.86; Found: C, 51.24; H, 5.20; N, 11.48. Conductivity = 349 μS/cm; μ_{eff} = 5.84 μ_B.

Chlorido-trans-[[2,2'-][(1,2-cyclohexanediyl) bis(nitrilomethylidyne)] bis[4-((1-ethylimidaz-olium)methylene)-phenolato]-[N,N',O,O'] iron(III) dichloride dihydrate (**6b**$\cdot 2H_2O$): Brown powder (484 mg, 73 %). FT-IR (KBr, cm^{-1}): FT-IR (KBr, cm^{-1}): 3433 (s, br, *v* O-H H_2O), 3136 (w, br, v_{asym} CH, CH, Im and Ph), 3068 (m, br, v_{sym} CH, Im and Ph), 2935 (m, sh, *v* CH_3), 2861 (m, sh, *v* CH_2), 1622 (vs, sh, *v* C=N), 1559, 1507, 1443 (s, sh, *v* $C=C_{arom}$ + *v* C-H bend), 1347 (m, sh, *v* CH_2), 1271 (m, sh, *v* Ph-O), 1152 (s, sh, HCC, HCN bending, Im), 832

(m, sh, *v* Fe-N), 468 (m, sh, *v* Fe-O). MALDI-TOF MS, *m/z*: 758.2 [M·2H_2O+Na]. Anal. Calcd. for $C_{32}H_{38}Cl_3FeN_6O_2$·2H_2O (M = 736.92): C, 52.16; H, 5.74; N, 11.40; Found: C, 52.26; H, 5.53; N, 11.11. Conductivity = 331 μS/cm; μ_{eff} = 5.80 μ_B.

Chlorido-trans-[[2,2'-][(1,2-cyclohexanediyl) bis(nitrilomethylidyne)] bis[4-((1-butylimidaz-olium)methylene)-phenolato]-[N,N',O,O'] iron(III) dichloride dihydrate (**6c**·~2H_2O): Dark-red powder (507 mg, 71 %). FT-IR (KBr, cm^{-1}): 3432 (m, br, *v* O-H H_2O), 3132 (w, br, v_{asym} CH, CH, Im and Ph), 2933 (m, sh, *v* CH_3), 2861 (m, sh, *v* CH_2), 1616 (vs, sh, *v* C=N), 1545, 1504, 1447 (s, sh, *v* C=C_{arom} + *v* C-H bend), 1350 (m, sh, *v* CH_2), 1270 (m, sh, *v* Ph-O), 1154 (s, sh, HCC, HCN bending, Im) , 822 (m, sh, *v* Fe-N), 463 (m, sh, *v* Fe-O). MALDI-TOF MS, *m/z*: 821.5 [M·~2H_2O+Na]$^+$. Anal. Calcd. for $C_{36}H_{46}Cl_3N_6O_2$·~2H_2O (M = 793.02): C, 54.52; H, 6.36; N, 10.60; Found: C, 54.11; H, 6.41; N, 10.51. Conductivity = 303 μS/cm; μ_{eff} = 5.78 μ_B.

Chlorido-trans-[[2,2'-][(1,2-cyclohexanediyl) bis(nitrilomethylidyne)] bis[4-((2-methylimidaz-olium)methylene) -6-(t-Bu-phenolato]-[N,N',O,O'] iron(III) dichloride dihydrate (**6d**·2H_2O): Dark-red solid (584 mg, 79 %). FT-IR (KBr, cm^{-1}): 3387 (m, br, *v* O-H H_2O), 3293 (m, br, *v* N(1)-H), 2995 (w, br, v_{asym} CH, CH, Im and Ph), 2941 (m, sh, *v* CH_3), 2860 (m, sh, *v* CH_2), 1619 (vs, sh, *v* C=N), 1567, 1478, 1443 (s, sh, *v* C=C_{arom} + *v* C-H bend), 1358 (m, sh, *v* CH_2), 1291 (m, sh, *v* Ph-O), 1145 (s, sh, *v* HCC + *v* HCN bending, Im), 801 (m, sh, *v* Fe-N), 442 (m, sh, *v* Fe-O). MALDI-TOF MS, *m/z*: 821.7 [M·2H_2O+H]$^+$. Anal. Calcd. for $C_{38}H_{50}Cl_3FeN_6O_2$·2H_2O (M = 821.08): C, 55.59; H, 6.63; N, 10.24; Found: C, 56.00; H, 6.71; N, 9.88. Conductivity = 323 μS/cm; μ_{eff} = 5.76 μ_B.

Chlorido-trans-[[2,2'-][(1,2-cyclohexanediyl) bis(nitrilomethylidyne)] bis[4-((1-ethylimidaz-olium)methylene) -6-(t-Bu-phenolato]-[N,N',O,O'] iron(III) dichloride dihydrate (**6e**·2H_2O): Dark-red solid (588 mg, 77 %). FT-IR (KBr, cm^{-1}): 3389 (m, br, *v* O-H H_2O), 3280 (m, br, *v* N(1)-H), 2998 (w, br, v_{asym} CH, CH, Im and Ph), 2953 (m, sh, *v* CH_3), 2865 (m, sh, *v* CH_2), 1617 (vs, sh, *v* C=N), 1566, 1476, 1445 (s, sh, *v* C=C_{arom} + *v* C-H bend), 1357 (m, sh, *v* CH_2), 1296 (m, sh, *v* Ph-O), 1144 (s, sh, *v* HCC + *v* HCN bending, Im), 800 (m, sh, *v* Fe-N), 438 (m, sh, *v* Fe-O). MALDI-TOF MS, *m/z*: 887.6 [M·2H_2O+K]$^+$. Anal. Calcd. for $C_{40}H_{54}Cl_3FeN_6O_2$·2H_2O (M = 849.13): C, 56.58; H, 6.88; N, 9.90; Found: C, 56.56; H, 6.87; N, 9.70. Conductivity = 305 μS/cm; μ_{eff} = 5.74 μ_B.

Chlorido-trans-[[2,2'-][(1,2-cyclohexanediyl) bis(nitrilomethylidyne)] bis[4-((1-butylimidaz-olium)methylene) -6-(t-Bu-phenolato]-[N,N',O,O'] iron(III) dichloride monohydrate (**6f**·H_2O): Dark-red solid, (562 mg, 69 %). FT-IR (KBr, cm^{-1}): 3432 (m, br, *v* O-H H_2O),2997 (w, br, *v* CH, Im and Ph), 2948 (m, sh, *v* CH_3), 2875 (m, sh, *v* CH_2), 1625 (vs, sh, *v* C=N), 1559, 1476, 1443 (s, sh, *v* $C=C_{arom}$ + *v* C-H bend), 1361 (m, sh, *v* CH_2), 1291 (m, sh, *v* Ph-O), 1179 (s, sh, *v* HCC + *v* HCN bending, Im), 799 (m, sh, *v* Fe-N), 436 (m, sh, *v* Fe-O). MALDI-TOF MS, *m/z*: 909.9 $[M{\cdot}H_2O+Na]^+$. Anal. Calcd. for $C_{44}H_{62}Cl_3FeN_6O_2{\cdot}H_2O$ (Mw = 887.22): C, 59.56; H, 7.27; N, 9.47; Found: C, 59.77; H, 7.65; N, 9.21. Conductivity = 288 μS/cm; μ_{eff} = 5.68 μ_B.

2.3. Antimicrobial activity

The plate-hole diffusion method was employed for the determination of antimicrobial activities against the gram (+), gram (−) bacterial and fungal organisms. Broth micro-dilution method was used to determine the MICs (minimum inhibitory concentrations) for the free ligands and their complexes in H_2O against test organisms. All the tests were performed in duplicate and repeated twice. Modal values were selected. Each microorganism was seeded in tube with nutrient broth (NB) (1 cm^3) which was then homogenized in the tubes with 9 cm^3 of melted (45 ^oC) nutrient Agar (NA). The homogeneous suspensions were poured into Petri dishes and holes of 4 mm diameter were done in the cool medium. After cooling these holes, 100 μL of the investigated compounds solutions, with serial concentrations, were applied using a micropipette with the pathogens to be tested against. The plates were incubated for 72h hours at 37 °C for bacteria and 28 °C for fungi, after that the clear zone around the wells was measured as inhibition zones and the diameter of these zone of inhibition (mm) were measured accurately. The antibacterial activities were observed and measured using a transparent meter rule and recorded if the zone of inhibition was ≥10 mm [25]. Ampicillin, Antibacterial, and Amphotericin B, Antifungal, were employed as standard drugs

3. Results and Discussion

3.1. Chemistry

3.1.1. Ligands Synthesis

The syntheses of the six ligands **4a-f** is depicted in Scheme 2. The required starting materials salicylaldehyde-imidazolium chloride salts **2a,b** were synthesized starting from 2-substituted phenol following modified literature procedures [22,23,26]. Under extra dry conditions and using anhydrous magnesium dichloride as O-magnesiation reagent, 2-*tert*-

butylphenol was formylated selectively ortho to the hydroxy group by paraformaldehyde with triethylamine as base. The substituted salicylaldehydes **1a,b** were then one-pot chloromethylated by reaction with paraformaldehyde and 37% HCl under a stream of HCl_g in the presence of catalytic amount of $ZnCl_2$ or tetrabutylammonium bromide at room temperature to yield 5-chloromethylated salicylaldehydes **2a,b** in a high purity. Modifying the R^1-group from hydrogen to a bulky t-butyl group increases the reaction time for chloromethylation at the 5-position from 1-3 days. Subsequent quarternization of alkylimidazole with **2a,b** generate salicylaldehyde-imidazolium chloride salts **3a-f**, which are the key intermediates in the synthesis of the achiral ligands. The chelating salts, (*rac-trans*-$H_2(R^1)_2$saldach$(Im^+\text{-}R^2R^3\text{-}Cl^-)_2$) **4a-f**, containing saldach skeleton were synthesized through the Schiff-base condensation reaction of compounds **3a-f** with (±)-*trans*-1,2-diaminocyclohexane (*rac-trans* dach) in methanolic solution. The *rac-trans* configuration of *N,N′*-bis(salicylidene)-1,2-cyclohexanediamine (saldach) backbone was chosen, because it forces the ligand into a flat chair (planar) conformation similar to the 1,2-cyclohexanediamine moiety present in oxaliplatin, a very promising metal-based drug [27]. Ligands were isolated in high yields, gave satisfactory elemental analysis, and characterized by spectroscopic techniques: ^{1}H NMR, ^{13}C NMR, FTIR, MALDI-TOF and conductivity measurements.

3.1.2. Synthesis of the Metallosaldach-Imidazolium Chlorides

Mn(III)-saldach-imidazolium chloride, synthesized by reaction of free ligands $H_2(R^1)_2$saldach$(Im^+\text{-}R^2R^3\text{-}Cl^-)_2$ (**4a-f**) and manganese(II) acetate tetrahydrate in 1 : 1 molar ratio in UV-methanol in a Schlenk line under nitrogen atmosphere followed by aerobic oxidation in the presence of LiCl, are dark brown glassy solids. Fe(III) complexes **6a-f** were obtained by the reaction of equimolar free saldach ligands with iron(III) chloride hexahydrate under anaerobic conditions (Scheme 3). All the synthesized compounds are soluble in water and most organic solvents. The resulting chelate complexes are highly soluble in common organic solvents and were fully characterized using the elemental analyses and spectroscopic techniques FTIR, UV-Vis, MALDI-TOF, ESI-MS as well as conductivity and magnetic measurements.

Unfortunately, all attempts to obtain X-ray diffraction quality single crystals of the Mn(III)- and Fe(III)-saldach-imidazolium chlorides ((**5,6)a-f**) were unsuccessful. Nevertheless, the metal-ligand structures suggested in this work (based upon elemental and

spectral analysis) match with the structures of reported metal-saldach analogues (Table S1, supporting information).

3.2. Characterization of free ligands and their complexes

The molar conductance values of the ligands and their complexes ranging from 220-284 and 288-351 μS/cm, respectively, reveal their electrolytic nature.

3.2.1. ^{1}H NMR studies

The most remarkable feature of the ^{1}H NMR spectra for all ligands is the down field singlet at 13.75-13.30 ppm which is assigned to the resonance of phenol OH [28,29]. The N-H of the imidazolium moiety in **4a,d** appears as a singlet at 9.48 and 10.05 respectively. The signal for the azomethine (CH=N) proton is observed at δ 8.68-8.28 ppm. Also, all saldach-imidazolium salts have two sets of resonance signals located in the aromatic region of the NMR spectrum (7.58-6.84 and 7.79-7.38 ppm) assigned to phenyl and imidazole protons, respectively. The signal set in the high-field region (4.00-3.43 and 1.85-1.42 ppm) is ascribed to the aliphatic cyclohexyl protons. To the best of our knowledge, the central saldach backbone is in the *O*-protonated tautomeric form not in the *N*-protonated tautomeric form (cf. Scheme 1) [32].

3.2.2. FTIR spectra

The selected IR spectra of the Schiff bases and their metal complexes along with their tentative assignments are reported in Table S2 (supporting information). In order to identify the IR signatures of the central saldach backbone, the bands caused by the terminal imidazolium compartments of saldach-imidazolium chloride have to be identified. The characteristic functionalities of saldach-imidazolium ligands include the hydrogen bonded hydroxyl groups, the azomethine groups (-C=N-) and the terminal imidazolium compartments. These functional groups were identified in by comparing the spectroscopic data with literature values of similar systems. Broad peaks were observed around ~ 3400 cm^{-1} in their IR spectra which strongly suggested the presence of intramolecular hydrogen bonding OH group. Additionally, a band at 1280-1253 cm^{-1} was assigned to a mixed ν(Ar-O).

H_2saldach and H_2(2-^{t}Bu)$_2$saldach exhibit a C=N stretch at 1639 and 1641 cm^{-1}, respectively [30,31]. Introduction of an imidazolium group in (**4a-f**) results in a low-energy shift to 1635-1629 cm^{-1}. This low-energy shift of the azomethine band by introduction of imidazolium group reflects the C=N bond order reduction induced by the (-I) effect of

quaternary N-atom and hydrogen bond with o-hydroxyl group [32]. The vibrational bands at ~846 and ~760 cm^{-1} should be assigned to the in-plane and out-of plane flexural vibration mode of the imidazolium ring respectively [33].

Formation of the complexes and their possible geometries were assigned on the basis of the electronic and infrared spectral studies, where in the absence of more powerful techniques such as X-ray, the FTIR data confirm its usefulness in the characterization of the coordination environments of these complexes ((**5,6)a-f**). So the study of the IR spectral data was quite informative in characterizing the metal-saldach binding modes.

All complexes exhibit very similar infrared spectral features. When comparing the spectroscopic data of Mn(III) and Fe(III) complexes with those of the free ligands, marked changes may be noticed in the ligand bands arising from various modes of donor groups involved in bonding to manganese and iron ions (Figure 1). The diagnostic IR spectral bands with their assignments of the free ligands and their metal complexes are shown in (cf Table S1, supporting information). The IR stretching bands due to azomethine *ν*(HC=N) register a red-shift of 11-15 and 10-17 cm^{-1} in the manganese(III)- and iron(III)-saldach-imidazolium complexes respectively (see Table 1) thus, indicating the coordination of the azomethine nitrogen to Mn(III) and Fe(III) ions [34], which is further confirmed by the appearance of a new band in the spectra of chelates at 543–570 cm^{-1} assigned to a νM(III)–N vibration (M= Mn, Fe) [35].

Strong bands attributable to phenolic oxygen *ν*(Ar–O) are evident ; these all show a shift of 9-17 and 7-21 cm^{-1} to higher energy in the manganese(III)- and iron(III) complexes from the free ligand values indicative of co-ordination to Mn(III) and Fe(III) respectively [35a]. The new IR band (456-475 cm^{-1}) is assigned to M-O vibrations [35a,36] and supports the ligation of the phenolate oxygen to metal ions. Moreover the disappearance of the phenolic O–H vibration, originally found in the saldach-imidazolium salts, indicates that it is deprotonated in complexes.

The bands ascribed to the vibration of the imidazole ring remain unchanged in the Mn(III) and Fe(III) complexes revealing that, the nitrogen atom of the imidazole moiety does not take part in metal coordination [37]. Finally, very broad bands centered at ca. 3430 and 3386 and 3424 cm^{-1} in some complexes can be assigned to the *ν* (OH) modes of lattice water in the corresponding framework [38].

These IR spectral studies reveal that the ligand coordinates to the metal ion in a tetradentate fashion through the deprotonated phenolate oxygen and azomethine nitrogen atoms (*i.e* with NONO (N_2O_2) donor sites).

3.2.3. Electronic Absorption Spectroscopy and magnetic susceptibility

The UV/Vis electronic spectra of the M(III)-saldach-imidazolium chloride complexes (M = Mn, Fe) (**5a-f**) (Table S3, supporting information) exhibit similar features, where all display a shoulder and three intense absorption peaks at ranges (266-272, 306-311, 393-395, 500-508) and (258-263, 299-304, 381-384, 504-511) for Mn(III) and Fe(III) complexes, respectively, which are assigned to the intra- and inter-ligand charge transfer and d-d transition. The higher energy band (< 300 nm) is due to intra-ligand π→π* transitions (*π→π**, LLCT), (phenyl and C=N moieties) [39]. Also higher energy bands (300-500 nm) are attributable to n→π* (phenolic oxygen) intra-ligand transitions. The most important feature in the near-UV region of the M(III)-saldach-imidazolium chloride is the higher wavelength band at (500-511 nm). These bands indicate the coordination of metal ion with the ligands, and this can be assigned to a charge-transfer band (MLCT), a transition from pπ orbitals on the phenolate oxygen atom to the dπ* orbitals of M(III) [40]. These bands in addition to a low intensity broad absorption bands (that may appear as shoulders > 600 nm) assigned to the three allowed d–d transitions expected for complexes with a square pyramidal geometry, ($d_{xz}\rightarrow d_{x2-y2}$), ($d_{xy}\rightarrow d_{x2-y2}$, d_{yz}) and ($d_{z2}\rightarrow d_{x2-y2}$) [41]. The magnetic moment values for the complexes (4.86-4.97 μ_B for Mn(III) saldach and 5.68-5.84 μ_B Fe(III) saldach) are also supportive of square pyramidal geometry with high spin metal centers.

One can clearly observe the effect of the substitution of the H-atom in [M(III)Cl{$(H)_2$saldach(Im^+-R^2R^3-$Cl^-)_2$}] (M= Mn, Fe; (**5,6**)**a-c**) with the *tert*-butyl group [M(III)Cl{$(^tBu)_2$saldach(Im^+-R^2R^3-$Cl^-)_2$}] (M= Mn, Fe;(**5,6**)**d-f**) upon UV absorption. The intensity of the two higher energy bands increased considerably as a result of enhancement the inter- and intra-ligand charge transfers. Also, the substitution shifts the absorption energy bands gradually to longer wavelengths. This effect is indicative of ligand *π-dπ* interactions between the saldach-imidazolium systems and the metal ion, which destabilize the ligand *π* molecular orbitals and decrease the *π-π** energy gap, thus producing a bathochromic shift.

3.3. Antimicrobial Screening

3.3.1. Antibacterial activity

The free ligands (saldach-imidazolium chlorides, **4a-f**), their metal complexes (Mn(III)-saldach-imidazolium chlorides, **5a-f** and Fe(III)-saldach-imidazolium chlorides, **6a-f**) and the standard drug Ampicillin ($C_{16}H_{19}N_3O_4S$, 349.41 $g \cdot mol^{-1}$) were screened separately for their antibacterial activity against the bacteria Staphylococus aureus (*S. aureus*, ATCC-25923) and Bacillus subtilis (*B. subtilis*, Re-cultured) (as gram-positive bacteria) and Pseudomonas aeruginosa (*P. aeruginosa*, ATCC-27853) and Eschercia coli (*E. coli*, ATCC-25922) (as gram-negative bacteria) at 2.5, 5, 10 and 20 mg/mL concentrations. The diffusion agar technique was used to evaluate the antibacterial activity of the synthesized compounds [42]. As a parameter of antibacterial activity, the MIC values were determined from the percentages of inhibition at four different concentration levels. From the bactericidal activity data Table S4 (supporting information), it has been observed that the ligand as well as its complexes shows a significant degree of antibacterial activity against G^+ bacteria (*S. aureus*, *B. subtilis*) and *E. coli* from G^- bacteria while slight activity or no activity toward *P. aeruginosa*. Generally it is apparent that, all compounds were more toxic towards gram positive strains than gram negative strains. This could be ascribed to their cell-wall structural differences, where the walls of gram negative species are more complex than those of gram positive cells, so it might be difficult for the compounds to diffuse inside the G^--bacterial cell. The zones of inhibition (ZOI) values are susceptible to the concentration of the compound used for inhibition (Figure S1, supporting information). The activity is greatly enhanced at the higher concentration. The ZOI values obtained indicate that the ligands have moderate to high activities as compared to Ampicillin drug towards the infection organisms (*S. aureus*, *B. subtilis*, *E. coli*). *N*,*N*'-Bis[3-*tert*-butyl-5-((2-methylimidazolium)methylene)-salicylidene)]-*trans*-1,2-cyclohexane-diamine dichloride (**4d**) and its Fe(III) complex (**6d**) exhibit remarkable extra-potent bactericidal activity (Figure 2), higher than the standard drug. Moreover, their MIC values are quite small. The MIC values Table 2 for ligand (**4d**) against *S. aureus*, *B. subtilis* and *E. coli* were 14.88, 12.14, and 13.30 µg/mL while for complex (**6d**) assigned 8.74, 10.33, and >250 µg/mL and, thus, can be classified as a new good candidate in the fight against bacterial infections.

Nature of the cell wall, the ligand, coordination sites, geometry of the compound, the positive charge density, hydrophilicity, lipophilicity, presence of co-ligand, pharmacokinetic factors, etc. also play decisive roles in determining antimicrobial activity of the Schiff base and its metal complexes [43]. These factors may affect the Fight against bacterial infections in two different ways: (i) interactions of compound with microbial cell wall, whereas the

cationic charges on the imidazolium enhance the bactericidal activity, which is partially credited to the electrostatic attraction between the positively charged ligand or complex and negatively charged cells walls [43]. (ii) Ability of tested compound to penetrate cell walls by simply dissolving into and through the lipophilic cell wall, recent results indicate that hydrophobic groups may increase the antimicrobial activity [44]. The variation in the antimicrobial activity of different compounds against different microorganisms depends on their impermeability of the cell or the differences in ribosomes in microbial cell [45]. The lipid membrane surrounding the cell favors the passage of any lipid soluble materials and it is known that lipophilicity is an important factor controlling antimicrobial activity [46]. In the present study, low activity of the some metal complexes is due to their low lipophilicity, because of which penetration of the complex through the lipid membrane was decreased and hence, they could neither block nor inhibit the growth of the microorganism.

From the data it has been also observed that the activity depends upon the type of metal ion and varies in the following order of the metal ion: Fe > Mn.

3.3.2. Proposed mechanisms of bactericidal action

A major component of a bacterial cell wall is peptidoglycan, that is, polysaccharide chains of alternating N-acetylglucosamine (NAG) and N-acetylmuramic acid (NAM) molecules that are cross-linked by peptide bonds between NAM subunits [47].

There are no recent studies of the mechanisms of bactericidal action of Schiff bases. Earlier work had suggested that the bacterial cell wall was a major target site [43b], especially the major wall component, peptidoglycan. Where the Schiff base and its complex indulge in the formation of hydrogen bonded interaction through the coordinated anion, hydroxyl group, etc. with the active centers of the microbial cell constituents resulting in interference with the normal cell processes.

Also saldach-imidazolium chlorides and their complexes may inhibit the peptidoglycan formation by irreversibly binding to the enzymes that cross-link NAM subunits and preventing the cross-linkage of NAM subunits (Figure 3).

3.3.3. Antifungal activity

The free ligands (**4a-f**), M(III) complexes ((**5,6**)**a-f**) and standard Antifungal drug (Amphotericin B, $C_{47}H_{73}NO_{17}$) were subjected for *in vitro* antifungal studies against Aspergillus flavus (*A. flavus*) Candida albicans (*C. albicans*, NCIM No. 3100) at 2.5, 5, 10

and 20 mg/mL concentration. From the experimental data Table S4 (supporting information), all saldach-imidazolium chlorides and their Fe(III) salts exhibited moderate antifungal activity against *C. albicans* infection, and the ZOI values slight increase as the concentration of tested compound raised from 2.5 to 20 mg/mL. However, they could not inhibit the growth of the *A. flavus*. None of the Mn(III)-saldach-imidazolium chloride salts has shown any observable activity against each fungal species. All tested compounds are infective against fungal strains. These limited or lack of fungicidal activity could be attributed to two possibilities: (i) the complex structure of fungal cell-wall, composed typically of chitin, 1,3-β- and 1,6-β-glucan, mannan and proteins [48], which could neither diffuse nor decrease the rate of diffusion of tested compound through. (ii) Fungal fighting proceed by much more complex mechanisms than bacterial conflict. Compound (**4d**) was identified as the most active against *C. albicans*.

Acknowledgment.

This work was in part supported by DFG grant Ja466/24-1 (initiation of bilateral cooperation RFME-CJ).

Appendix A. Supplementary material

Supplementary data (FT-IR spectral data, UV/Vis Spectral Data and antimicrobial evaluation) associated with this article can be found, in the online version, at doi: 10.1016/ j.ejmech. XXXXXXXX

References

[1] A. Tanitame, Y. Oyamada, K. Ofuji, M. Fujimoto, K. Suzuki, T. Ueda, H. Terauchi, M. Kawasaki, K. Nagai, M. Wachi, J. Yamagishi, Bioorg. Med. Chem. 12 (2004) 5515-5524.

[2] D.T. Chu, J.J. Plattner, L. Katz, J. Med. Chem. 39 (1996) 3853-3874.

[3] R. S. Levings, D. Lightfoot, S. R. Partridge, R. M. Hall, S. P. Djordjevic, J. Bacteriol. 187 (2005) 4401-4409.

[4] C. Schnellmann, V. Gerber, A. Rossano, V. Jaquier, Y. Panchaud, M. G. Doherr, A. Thomann, R. Straub, V. Perreten, J. Clin. Microbiol. 44 (2006) 4444-4454.

[5] J.R. Govan, V. Deretic, Microbiol. Rev. 60 (1996) 539-574.

[6] L. Ballell, R.A. Field, K. Duncan, R.J. Young, Antimicrob. Agents Chemother. 49 (2005) 2153-2163.

[7] J.F. Barrett, J.A. Hoch, Antimicrob. Agents Chemother. 42 (1998) 1529-1536.

[8] T. Miyamoto, J. Matsumoto, K. Chiba, H. Egawa, K. Shibamori, A. Minamida, Y. Nishimura, H. Okada, M. Kataoka, M. Fujita, T. Hirose, J. Nakano, J. Med. Chem. 33 (1990) 1645-1656.

[9] N. Nakada, H. Shimada, T. Hirata, Y. Aoki, T. Kamiyama, J. Watanabe, M. Arisawa, Biological characterization of cyclothialidine, Antimicrob. Agents Chemother. 37 (1993) 2656-2661.

[10] I. Correia, J.C. Pessoa, M. Teresa Duarte, M.F. Minas da Piedade, T. Jackush, T. Kiss, M.M.C.A. Castro, C.F.G.C. Geraldes, F. Avecilla, Eur. J. Inorg. Chem. (2005) 732–744.

[11] D. Barton, W.D. Ollis, Comprehensive Organic Chemistry, vol. 2, Pergamon Oxford, (1979).

[12] (a) R.W. Layer, The Chemistry of Imines, Chem. Rev. 63 (1963) 489–510; (b) H. Tanaka, A. Ağar, M. Yavuz, J. Mol. Model. 16 (2010) 577-587.

[13] P.A. Vigato, S. Tamburini, Coord. Chem. Rev. 248 (2004) 1717-2128.

[14] B. M. Drašković, G. A. Bogdanović, M. A. Neelakantan, A.-C. Chamayou, S. Thalamuthu, Y. S. Avadhut, J. Schmedt auf der Günne, S. Banerjee, C. Janiak, Cryst. Growth Des. 10 (2010) 1665-1676.

[15] L. Shi, W.-J. Mao, Y. Yang and H.-L. Zhu, J. Coord. Chem. 62 (2009) 3471-3477.

[16] M.A. Phaniband, S.D. Dhumwad, Transit. Met. Chem. 32 (2007) 1117-1125.

[17] G. Kumar, S. Devi, R. Johari, E-Journal of Chemistry 9 (2012) 2119-2127.

[18] F. Pfannkuch, H. Rettig, P. H.Stahl, C. G. Wermuth, P. H. Stahl, Handbook of Pharmaceutical Salts: Properties, Selection, and Use, Wiley-VCH: Weinheim, Germany, (2002) p 130.

[19] (a) J. Pernak, K. Sobaszkiewicz, I. Mirska, Green Chem. 2003, 5, 52; (b) J. Pernak, I. Goc, I. Mirska, Green Chem. 6 (2004) 323-329; (c) M.T. Garcia, N. Gathergood, P.J. Scammells, Green Chem. 7 (2005) 9-14; (d) P.J. Scammels, J.L. Scott, R.D. Singer, Aust. J. Chem. 58 (2005) 155-169; (e) N. Gathergood, P.J. Scammels, Aust. J. Chem. 55 (2002) 557-560; (f) J. Łuczak, C. Jungnickel, I. Łacka, S. Stolte, J. Hupka, Green Chem. 12 (2010) 593-601.

[20] S. V. Malhotra, V. Kumar, Bioorg. Med. Chem. Lett. 20 (2010) 581-585.

[21] (a) R. F. El-Shaarawy, Synthesis and reactions of some pyridoyl derivatives with anticipated biological activities, M.Sc. thesis, Suez Canal university, Egypt (2001); (b) B. Wisser, C. Janiak, Z. Anorg. Allg. Chem. 633 (2007) 1796-1800; (c) R.F. El-Shaarawy, H.K. Ibrahim, E. Eltamany, I. Mohy-Eldeen, Maced. J. Chem. Chem. Eng. 27 (2008) 65-79; (d) A.-C. Chamayou, M. A. Neelakantan, S. Thalamuthu, C. Janiak, Inorg. Chim. Acta 365 (2011) 447-450. (e) R.F.M El-Shaarawy, C. Janiak, I.M. El-Deen, E.H. El-Tamany, J. Mol. Struct. (2013) submitted.

[22] G. Casiraghi, G. Casnati, M. Cornia, A. Pochini, G. Puglia, G. Sartori, R. Ungaro, J. Chem. Soc. Perkin Trans. 1 (1978) 318-321.

[23] Y. Yang, J.Q. Guan, P.P. Qiu, Q.B. Kan, Transit. Met. Chem. 35 (2010) 263–270

[24] L. Canali, E. Cowan, H. Deleuze, C.L. Gibson, D.C. Sherrington, J. Chem. Soc. Perkin Trans. 1 (2000) 2055-2066.

[25] A.J. Vlietink, L. Van Hoof, J. Totte, H. Laure, D.V. Berhe, P.C. Rwangabo, J. Mrukiyunmwami, J. Ethnopharm. 46 (1995) 31-47.

[26] P.U. Naik, G.J. McManus, M.J. Zaworotko, R.D. Singer, Dalton Trans. (2008) 4834-4836.

[27] A. Hille, I. Ott, A. Kitanovic, I. Kitanovic, H. Alborzinia, E. Lederer, S. Wölfl, N. Metzler-Nolte, S. Schäfer, W.S. Sheldrick, C. Bischof, U. Schatzschneider, R. Gust J. Biol. Inorg. Chem. 14 (2009) 711-725.

[28] R. C. Felicio, E.T.G. Cavalheiro, E.R. Dockal, Polyhedron 20 (2001) 261-268.

[29] A. Clearfield, R. Gopal, R.J. Kline, M. Sipski, L.O. Urban, J. Coord. Chem. 7 (1978) 163-169.

[30] M.R. Mauryaa, A.K. Chandrakar, S. Chand, J. Mol. Cat. A 270 (2007) 225-235.

[31] P.J. Pospisil, D.H. Carsten, E.N. Jacobsen, Chem. Eur. J. 2 (1996) 974-980.

[32] C.-G.F. Richthofen, A. Stammler, H. Bögge, T. Glaser, J. Org. Chem. 77 (2012) 1435-1448.

[33] S. Tait, R.A. Osteryoung, Inorg. Chem. 23 (1984) 4352-4360.

[34] (a) Webster F.X., Silverstein R.M., "Spectrophotometer Identification of Organic Compounds", 6th ed., John Wiley, New York, 87 (1992); (b) O. Pouralimardan, A.-C. Chamayou, C. Janiak, H.H.-Monfared, Inorg. Chimica Acta 360 (2007) 1599-1608; (c) R. I. Kureshy, K. J. Prathap, T. Roy, N.C. Maity, N.H. Khan, S. H. R. Abdi, H.C. Bajaj, Adv. Synth. Catal. 352 (2010) 3053-3060; (d) T. Chang, L.Jin, H. Jing, ChemCatChem 1 (2009) 379-383.

[35] (a) Nakomoto K., "Infrared and Raman Spectroscopy of Inorganic and Coordination Compounds", 3rd ed., Wiley Interscience, New York (1978); (b) G. Karimipour, M. Montazerozohori, N.H. Naeini, Iran. J. Chem. Chem. Eng. 30 (2011) 13-18; (c) X. Guojin, W. Saili, F. Yingguo, Z. Libo, T. Yuhai, Z. Yuansuo, Chin. J. Catal. 33 (2012) 473-477.

[36] G.B. Pethe, A.R. Yaul, J.B. Devhade, A. S. Aswar, Der Pharma Chemica. 2 (2010) 301-308.

[37] J. Huang, X. Fu, G. Wang, Q. Miao, G. Wang, Dalton Trans. 41 (2012) 10661-10669.

[38] K. Nakamato, Infrared and Raman Spectra of Inorganic and Coordination Compounds, 4th ed., Wiley, New York (1986) p. 242.

[39] A. Silva, C. Freire, B. de Castro, New J. Chem. 28 (2004) 253-260.

[40] L.J. Boucher, M.O. Farrell, J. Inorg. Nucl. Chem. 35 (1973) 3731-3738.

[41] B. P. Gaber, V. Miskowski, T.G. Spiro, J. Am. Chem. Soc. 96 (1974) 6868-6873.

[42] A. Rahman, M.I. Choudhary, W.J. Thomsen, Bioassay Techniques for Drug Development, Harwood Academic Publishers, The Netherlands (2001) p 16.

[43] (a) M. Kong, X.G. Chen, K. Xing, H.J. Park, Int. J. Food Microbiol. (2010) 51-63. (b) V.P. Daniel, B. Murukan, B.S. Kumari, K. Mohanan, Spectrochim Acta A: Mol. Biomol. Spectrosc. 70 (2008) 403-410.

[44] E.I. Rabea, M.E.I Badawy, T.M. Rogge, C.V. Stevens, M. Höfte, W. Steurbaut, G. Smagghe, Pest. Manag. Sci. 61 (2005) 951-960.

[45] S.K. Sengupta, O.P. Pandey, B.K. Srivastava, V.K. Sharma, Transit. Met. Chem. 23 (1998) 349-353.

[46] G. Kumar, D. Kumar, C.P. Singh, A. Kumar, V.B. Rana, J. Serb. Chem. Soc. 75 (2010) 629-637.

[47] S. Fujii, H. Kumagai, M. Noda, Carbohydr. Res. 83 (1980) 389-393

[48] R.F. Hector, Clin. Microbiol. Rev. 6 (1993) 1-21.

Tables Captions

Table 1: Assignment of the vibrations that are Responsible for the FTIR from the free saldach ligands (**4a-f**) and their complexes ((**5,6**)**a-f**).

Table 2: Minimum inhibitory concentration (MIC) profiles of the saldach-imidazolium chlorides and their M(III) complexes against different strains

Table 1: Assignment of the vibrations that are Responsible for the FTIR from the free saldach ligands (**4a-f**) and their complexes ((**5,6**)**a-f**)

Compound	*ν* HC=N	Δ*ν* HC=N	*ν* O-H	*ν* Ar-O	Δ*ν* Ar-O	*ν* Imidazole	*ν* M-N	*ν* M-O
4a	1630	–	3395	1258	–	761	–	–
5a	1618	-12	–	1275	+17	760	570	475
6a	1617	-13	3408	1279	+21	759	569	471
4b	1632	–	3434	1253	–	760	–	–
5b	1621	-11	3426	1273	+20	761	547	471
6b	1622	-10	3433	1271	+18	760	543	468
4c	1629	–	3398	1260	–	760	–	–
5c	1614	-15	3436	1272	+12	759	545	468
6c	1616	-13	3432	1270	+10	760	544	463
4d	1629	–	3430	1281	–	770	–	–
5d	1616	-13	3411	1295	+14	771	568	482
6d	1619	-10	3387	1291	+10	769	564	478
4e	1634	–	3446	1285	–	770	–	–
5e	1622	-12	3388	1298	+13	770	559	463
6e	1617	-17	3389	1296	+11	771	555	458
4f	1635	–	3486	1284	–	768	–	–
5f	1623	-12	–	1293	+9	769	565	468
6f	1625	-10	3432	1291	+7	768	562	456

Table 2: Minimum inhibitory concentration (MIC) profiles of the saldach-imidazolium chlorides and their M(III) complexes against different strains

Sample	Minimum inhibitory concentration (**MIC**) (μgmL^{-1} sample)					
	Bacteria				**Fungi**	
	G^+ Bacteria		**G^+ Bacteria**			
	S. aureus	**B. subtilis**	**E. coli**	**P. aeruginosa**	**A. flavus**	**C. albicans**
4a	17.60	17.50	17.12	>10000	-ve	>250
5a	21.50	19.23	15.43	>10000	-ve	-ve
6a	14.85	16.03	**10.16**	>10000	-ve	>250
4b	> 250	15.24	> 250	>10000	-ve	>250
5b	> 250	15.62	18.38	>10000	-ve	-ve
6b	> 250	16.89	12.88	>10000	-ve	-ve
4c	16.23	11.16	16.66	>5000	-ve	>250
5c	21.18	15.41	18.65	>5000	-ve	-ve
6c	17.12	13.73	17.86	>5000	-ve	90.50
4d	14.88	12.14	13.30	>10000	-ve	**55.50**
5d	**11.90**	12.35	14.37	>5000	-ve	-ve
6d	**8.74**	**10.33**	> 250	>250	-ve	>250
4e	18.39	16.03	> 250	>10000	-ve	>250
5e	> 250	19.23	17.60	>10000	-ve	>250
6e	> 250	17.50	16.66	>10000	-ve	>250
4f	16.02	16.44	12.25	>5000	-ve	85.25
5f	21.18	18.38	16.23	>5000	-ve	-ve
6f	18.11	16.66	14.40	>250	-ve	>250
Ampicillin (Antibaterial drug)	**12.50**	**20.00**	**15.00**	**>1000**	-ve	-ve
Amphotericin B (Antifungal drug)	-ve	-ve	-ve	-ve	**40.00**	**80.00**

Figures Captions

Figure 1: Selected IR fragment, for comparison the azomethine and phenolate stretches and their splitting patterns from **4b, 5b and6b**.

Figure 2: Graph of zone of inhibition/mm for target compounds against different bacterial species.

Figure 3: Bacterial cell wall synthesis and the inhibitory effects of H_2saldach-Im chlorides and their complexes on it.

Figure 1: Selected IR fragment, for comparison the azomethine and phenolate stretches and their splitting patterns from **4b, 5b and6b**.

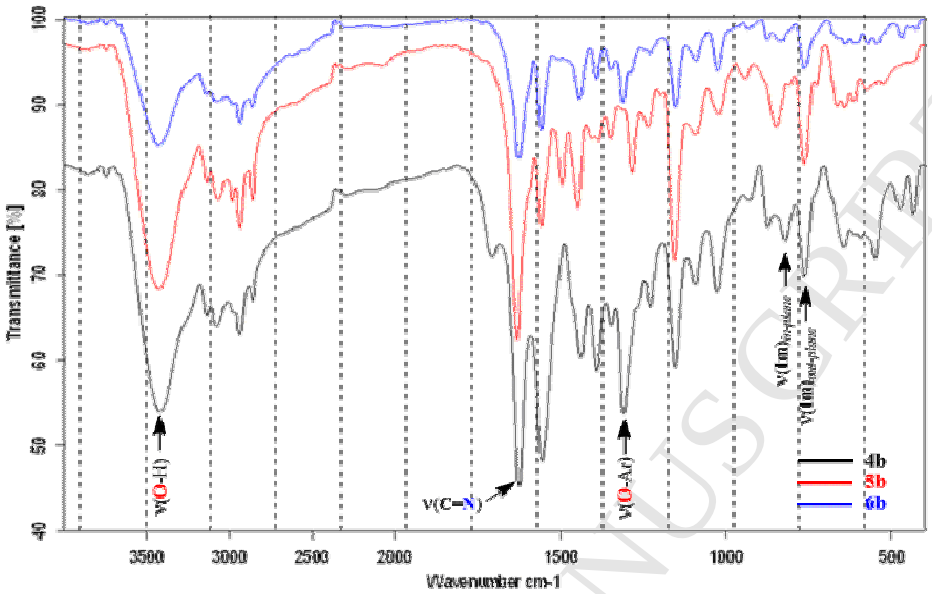

Figure 2: Graph of zone of inhibition/mm for target compounds against different bacterial species.

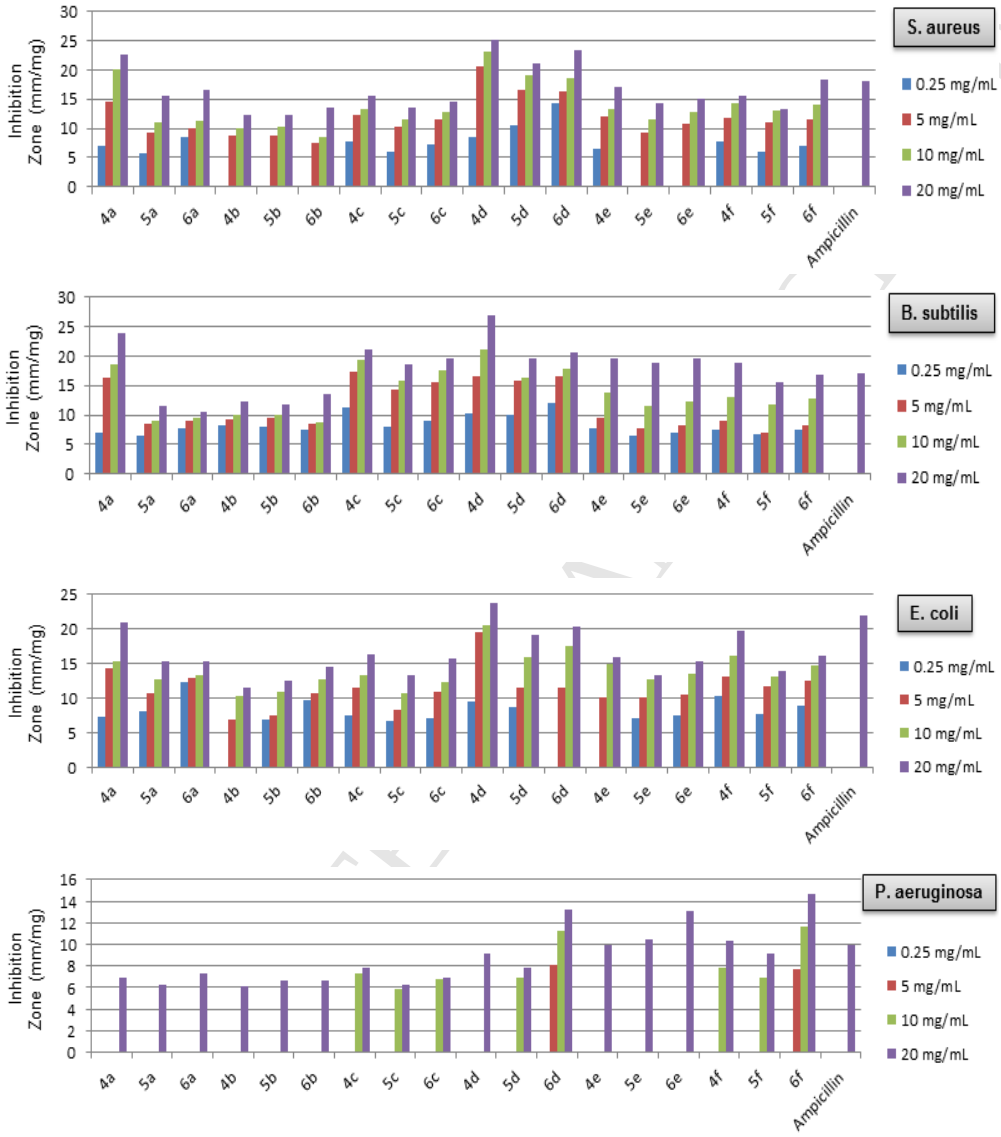

Figure 3: Bacterial cell wall synthesis and the inhibitory effects of H_2saldach-Im chlorides and their complexes on it. (a) A schematic depiction of a normal peptidoglycan cell wall showing NAG-NAM chains and cross-linked NAM subunits (normal cell walls). (d) A schematic depiction of the effect of free ligands and complexes on peptidoglycan in preventing NAM-NAM cross-links; (i) electrostatic attraction between the positively charged imidazolium moieties and negatively charged cells walls and then penetration by dissolution into and through the cell wall, (ii) Bacterial lysis due to the effects of the tested compounds.

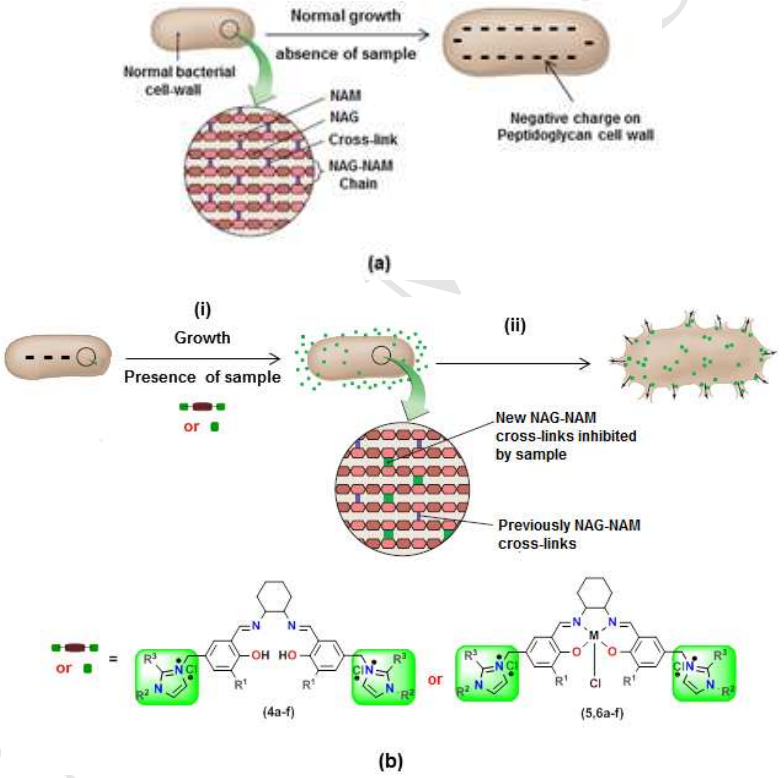

Schemes Captions

Scheme 1: Saldach-imidazolium chloride ligands with the tautomeric equilibrium and Mn(III)- and Fe(III)-saldach-imidazolium chloride complexes used in this work.

Scheme 2: Synthesis of salicylaldehyde- (**3a-f**) and saldach-imidazolium chloride salts, **4a-f**.

Scheme 3: Synthesis of Mn(III)- and Fe(III)-saldach-imidazolium chloride complexes, **5a-f** **6a-f**, respectively.

Scheme 1. Saldach-imidazolium chloride ligands with the tautomeric equilibrium and Mn(III)- and Fe(III)-saldach-imidazolium chloride complexes used in this work.

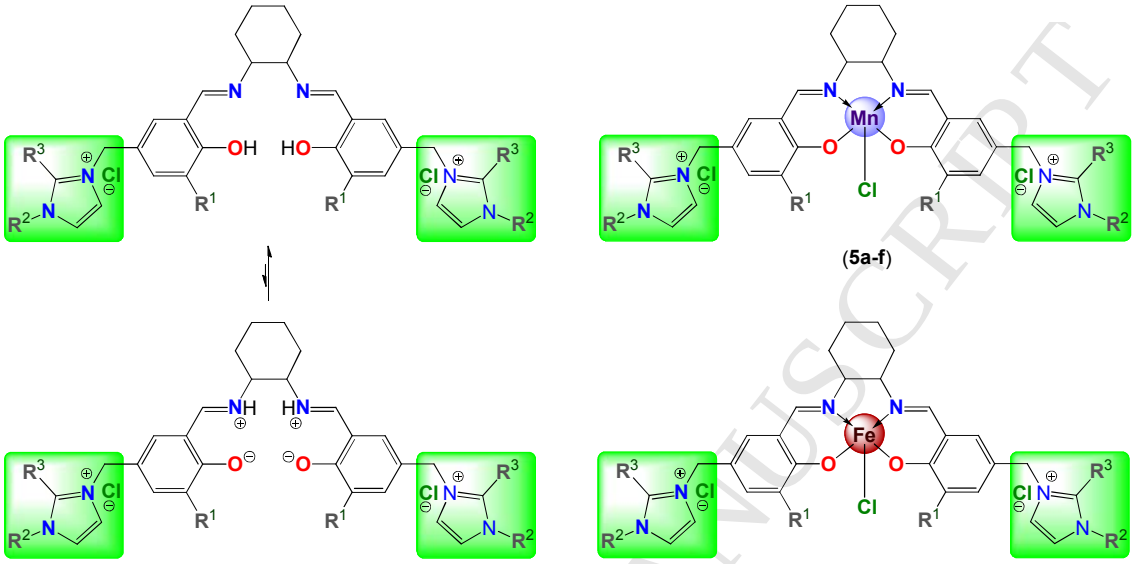

$H_2(R^1)_2$saldach(Im$^+$-R^2R^3-Cl^-)$_2$

a R^1= H, R^2=H, R^3=Me,
b R^1= H, R^2=Et, R^3=H
c R^1= H, R^2=*n*-Bu, R^3=H
d R^1=*t*-Bu, R^2=H, R^3=Me
e R^1=*t*-Bu, R^2=Et, R^3=H
f R^1=*t*-Bu, R^2=*n*-Bu, R^3=H

[M(III)Cl{(R^1)$_2$saldach(Im$^+$-R^2R^3-Cl^-)$_2$}]

Scheme 2. Synthesis of salicylaldehyde- (**3a-f**) and saldach-imidazolium chloride salts, **4a-f**.

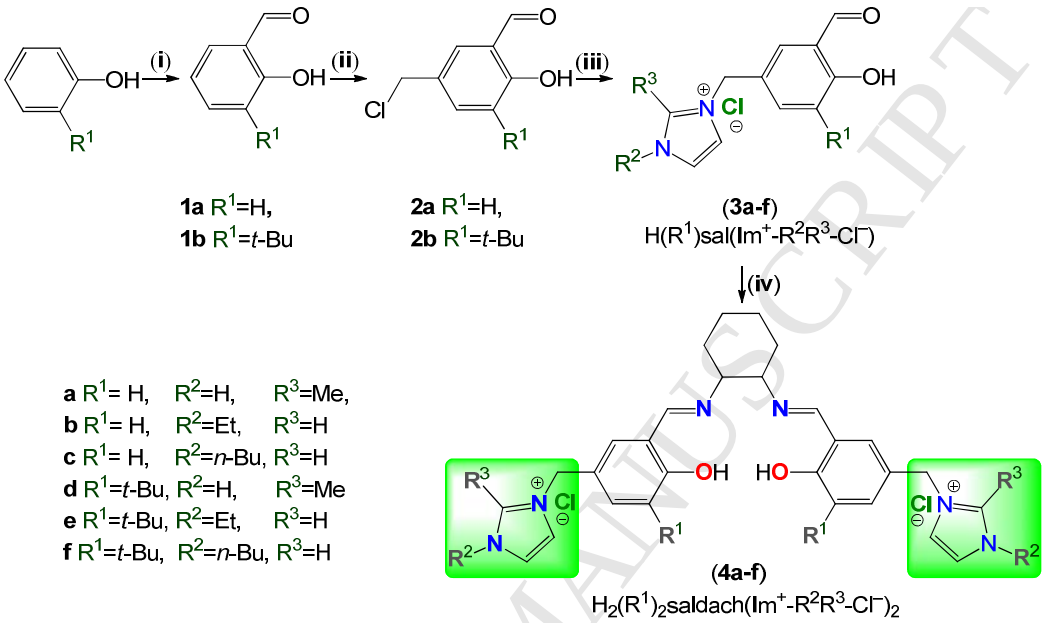

(**i**) 1. Anhydrous $MgCl_2$, $(CH_2O)_n$, Et_3N, ACN, stir, r.t; 2. HCl. (**ii**) CH_2O, $ZnCl_2$, HCl_{aq}, HCl_g, stir, r.t. (**iii**) Alkylimidazole, toluene, stir, 80 ^oC, N_2. (**iv**) MeOH, reflux, stir, N_2.

Scheme 3. Synthesis of Mn(III)- and Fe(III)-saldach-imidazolium chloride complexes, **5a-f** **6a-f**, respectively.

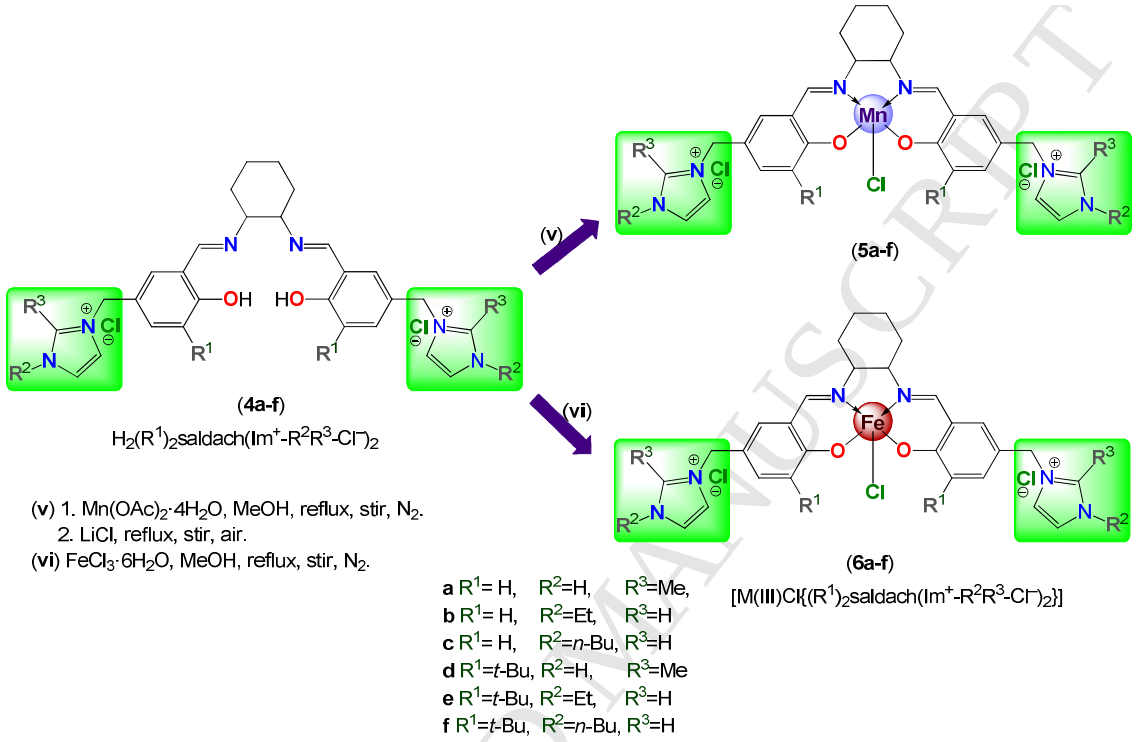

"**Toward new classes of potent antibiotics: synthesis and antimicrobial activity of novel metallo-saldach-imidazolium salts.** The previous title was

Reda F.M. Elshaarawy,[a,b,*] and Christoph Janiak[b,*]

[a] Faculty of Science, Suez University, Suez, Egypt. Email: reda_elshaarawi@science.suez.edu.eg; Reda.El-Shaarawy@uni-duesseldorf.de

[b] Institut für Anorganische Chemie und Strukturchemie, Heinrich-Heine Universität Düsseldorf, 40204 Düsseldorf, Germany. Email: janiak@uni-duesseldorf.de

Tables Captions

Table S1: Structures of some literature complex from CSD.

Table S2: FTIR Spectral Data with their assignments for the free ligands and their M(III)-complexes

Table S3: UV−Vis Spectral Data (λ_{max} in nm) for the M(III)-Saldach-imidazolium chlorides (**(5,6)a-f**)

Table S4: Inhibition zone (mm/mg sample) for the free ligands and their M(III)-complexes

Table S1: Structures of some literature complex from CSD

Entry	Structure	Reference
POYPIC	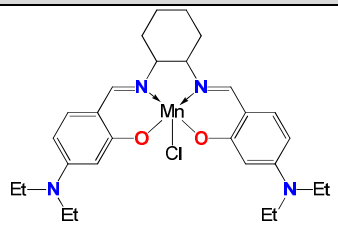	S1
TOVNIB01	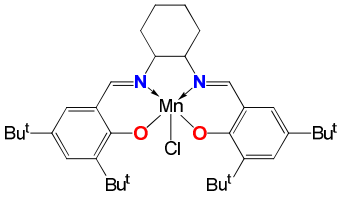	S2
XEMYAP	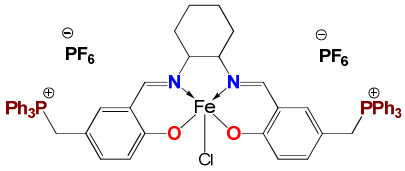	S3
AGIXOE	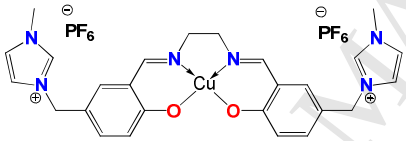	S4

Reference

S1. G. Lenoble, P.G. Lacroix, J.C. Daran, S.D. Bella, K. Nakatani, Inorg. Chem. 37 (1998), 2158.

S2. J.W. Yoon, T.-S. Yoon, S.W. Lee, W. Shin, Acta Crystallogr. Sect. C: Cryst. Struct. Commun. 55 (1999) 1766.

S3. A. Pajunen, I. Mutikainen, A. Haikarainen, J. Sipila; Z. Kristallogr. New Cryst.Struct. 216 (2001) 147

S4. P.U. Naik, G.J. McManus, M.J. Zaworotko, R.D. Singer; Dalton Trans. (2008), 4834.

Table S2: FTIR Spectral Data with their assignments for the free ligands and their M(III)-complexes

Sample	*ν* O-H	*ν* N-H	*ν* C=N	*ν* Ar-O	*ν* HCN Im	*ν* Im	*ν* M-N	*ν* M-O
Saldach-bis(MeImCl) (**4a**)	3395	3285	1630	1258	1160	761	–	–
Mn(III)Saldach-bis(MeImCl) (**5a**)	–	3286	1618	1275	1167	760	570	475
Mn(III)Saldach-bis(MeImCl) (**6a**)	3408	3290	1617	1279	1166	759	569	471
Saldach-bis(EtImCl) (**4b**)	3434	–	1632	1253	1155	760	–	–
Mn(III)Saldach-bis(EtImCl) (**5b**)	3426	–	1621	1273	1152	761	547	471
Mn(III)Saldach-bis(EtImCl) (**6b**)	3433	–	1622	1271	1152	760	543	468
Saldach-bis(^{n}BuImCl) (**4c**)	3398	–	1629	1260	1158	760	–	–
Mn(III)Saldach-bis(^{n}BuImCl) (**5c**)	3436	–	1614	1272	1152	759	545	468
Mn(III)Saldach-bis(^{n}BuImCl) (**6c**)	3432	–	1616	1270	1154	760	544	463
^{t}BuSaldach-bis(MeImCl) (**4d**)	3430	3295	1629	1281	1149	770	–	–
Mn(III) ^{t}BuSaldach-bis(MeImCl) (**5d**)	3411	3294	1616	1295	1142	771	568	482
Mn(III) ^{t}BuSaldach-bis(MeImCl) (**6d**)	3387	3293	1619	1291	1144	769	564	478
^{t}BuSaldach-bis(EtImCl) (**4e**)	3446	–	1634	1285	1138	770	–	–
Mn(III) ^{t}BuSaldach-bis(EtImCl) (**5e**)	3388	–	1622	1298	1136	770	559	463
Mn(III) ^{t}BuSaldach-bis(EtImCl) (**6e**)	3389	–	1617	1296	1145	771	555	458
^{t}BuSaldach-bis(^{n}BuImCl) (**4f**)	3486	–	1635	1284	1176	768	–	–
Mn(III) ^{t}BuSaldach-bis(^{n}BuImCl) (**5f**)	–	–	1623	1293	1178	769	565	468
Mn(III) ^{t}BuSaldach-bis(^{n}BuImCl) (**6f**)	3432	–	1625	1291	1179	768	562	456

Table S3. UV−Vis Spectral Data (λ_{max} in nm) for the M(III)-Saldach-imidazolium chlorides (**(5,6)a-f**)

Sample	**Electronic transitions**		
	π→ π*	n→π*	pπ→dπ*& d→d
Mn(III)Saldach-MeimCl (**5a**)	266	306, 393	500
Mn(III)Saldach-EtimCl (**5b**)	270	308,395	505
Mn(III)Saldach-^{n}BuimCl (**5c**)	272	311, 395	508
Fe(III)Saldach-MeimCl (**5d**)	258	299, 381	504
Fe(III)Saldach-EtimCl (**5e**)	261	303,383	509
Fe(III)Saldach-^{n}BuimCl (**5f**)	263	304, 384	511
Mn(III)^{t}Busaldach-MeimCl (**6a**)	279	324, 411	516
Mn(III)^{t}Busaldach-EtimCl (**6b**)	284	325,410	519
Mn(III)^{t}Busaldach-^{n}BuimCl (**6c**)	285	326,412	520
Fe(III)^{t}Busaldach-MeimCl (**6d**)	271	317, 395	538
Fe(III)^{t}Busaldach-EtimCl (**6e**)	275	325,397	543
Fe(III)^{t}Busaldach-^{n}BuimCl (**6f**)	275	325, 398	543

Table S4. Inhibition zone (mm/mg sample) for the free ligands and their M(III)-complexes

Sample	Diameter of inhibition zone (mm/mg sample)															
	G^+ Bacteria								G^- Bacteria							
	S. aureus				B. subtilis				E. coli				P. aeruginosa			
(mg/mL)	0.25	5	10	20	0.25	5	10	20	0.25	5	10	20	0.25	5	10	20
4a	7.1	14.5	20.2	22.6	7.1	16.3	18.5	**24.0**	7.3	14.3	15.4	20.9	-ve	-ve	-ve	6.9
5a	5.8	9.2	11.1	15.7	6.5	8.4	9.1	11.5	8.1	10.6	12.7	15.3	-ve	-ve	-ve	6.2
6a	8.4	10.1	11.2	16.5	7.8	8.9	9.5	10.6	12.3	12.8	13.4	15.4	-ve	-ve	-ve	7.3
4b	-ve	8.8	10.1	12.3	8.2	9.2	10.1	12.4	-ve	6.8	10.3	11.5	-ve	-ve	-ve	6.1
5b	-ve	8.7	10.2	12.2	8.0	9.4	10.1	11.9	6.8	7.5	10.8	12.4	-ve	-ve	-ve	6.6
6b	-ve	7.5	8.6	13.5	7.4	8.4	8.8	13.5	9.7	10.7	12.6	14.6	-ve	-ve	-ve	6.7
4c	7.7	12.4	13.4	15.6	11.2	17.3	19.3	21.2	7.5	11.4	13.3	16.4	-ve	-ve	7.3	7.8
5c	5.9	10.3	11.6	13.5	8.1	14.2	15.8	18.7	6.7	8.3	10.6	13.3	-ve	-ve	5.9	6.3
6c	7.3	11.5	12.7	14.5	9.1	15.5	17.6	19.6	7.0	10.8	12.2	15.8	-ve	-ve	6.8	6.9
4d	8.4	20.5	23.2	**25.2**	10.3	16.5	21.1	**26.9**	9.4	19.6	20.5	**23.8**	-ve	-ve	-ve	9.1
5d	10.5	16.7	19.1	21.1	10.1	15.8	16.4	19.7	8.7	11.4	15.9	19.2	-ve	-ve	6.9	7.8
6d	14.3	16.4	18.6	23.5	12.1	16.6	17.9	20.5	-ve	11.5	17.6	20.4	-ve	8.1	11.3	13.2
4e	6.6	12.1	13.3	17.1	7.8	9.5	13.8	19.6	-ve	10.1	14.9	16.0	-ve	-ve	-ve	9.9
5e	-ve	9.3	11.6	14.4	6.5	7.7	11.5	18.9	7.1	10.0	12.7	13.3	-ve	-ve	-ve	10.4
6e	-ve	10.8	12.9	15.0	7.1	8.2	12.2	19.6	7.5	10.5	13.6	15.3	-ve	-ve	-ve	13.1
4f	7.8	11.9	14.2	15.5	7.6	8.9	13.1	18.8	10.2	13.1	16.1	19.7	-ve	-ve	7.8	10.3
5f	5.9	11.1	13.1	13.3	6.8	7.1	11.9	15.6	7.7	11.7	13.2	14.0	-ve	-ve	6.9	9.1
6f	6.9	11.6	14.0	18.4	7.5	8.2	12.7	16.7	8.8	12.5	14.8	16.2	-ve	7.7	11.6	**14.7**
Ampicillin (Antibaterial drug)				18				17				22				10

Inspection for a new generation of highly potent antibiotics: a profile of the *in vitro* antimicrobial activity of novel metallosaldach-imidazolium salts

Reda F.M. Elshaarawy,[a,b,*] and Christoph Janiak[b,*]

[a] Faculty of Science, Suez University, Suez, Egypt. Email: reda_elshaarawi@science.suez.edu.eg; Reda.El-Shaarawy@uni-duesseldorf.de

[b] Institut für Anorganische Chemie und Strukturchemie, Heinrich-Heine Universität Düsseldorf, 40204 Düsseldorf, Germany. Email: janiak@uni-duesseldorf.de

Figure Captions

Figure S1: Antibacterial susceptibility tests of ^{t}-Busaldach-Im Cl (**4d**)against G^{+} bacteria.

Figure S1: Antibacterial susceptibility tests of ^{t}-Busaldach-Im Cl (**4d**)against G^{+} bacteria